THE RATIO OF π^0 PHOTOPRODUCTIONS FROM NEUTRONS AND PROTONS IN DEUTERIUM IN THE ENERGY RANGE OF 700 TO 1100 MEV

Thesis by

Tseng-Hsu Chang

In Partial Fulfillment of the Requirements

For the Degree of

Doctor of Philosophy

California Institute of Technology

Pasadena, California

1962

ACKNOWLEDGEMENTS

The present experiment was suggested and supervised by Professor Robert L. Walker. I am deeply indebted to him for his advice and encouragement during the course of the experiment.

I would like to thank Dr. Karl Althoff who started this experiment and Dr. G. Neugebauer who helped him during the early stages of this experiment. I would also like to thank Dr. Ricardo Gomez and Dr. Joe Mullins for many helpful discussions, and Mr. Richard Talman for discussions on the lead glass Cerenkov counter mentioned in Section VII.

The help of Mr. R. Diebold and Mr. W. Ing during several stages of this experiment is deeply appreciated. The synchrotron operators under the supervision of Mr. A. Neubieser admirably maintained the running of the synchrotron. The engineering staff, in particular Mr. D. Sell and Mr. E. Taylor, and the crew of the synchrotron under the supervision of Mr. L. Loucks gave continued assistance.

I would like to thank Mrs. Sharon Reed who did most of the scanning, and other scanners whose patience and effort made the task of scanning possible.

Partial support of the Atomic Energy Commission and the interest of Dr. R. F. Bacher are gratefully acknowledged.

ABSTRACT

The ratio of the cross sections for photoproduction of neutral pions from neutrons to that from protons has been obtained at average photon energies of 750, 875, and 1050 mev at a pion CM angle of 60^{o} and at average photon energies of 875 and 1050 mev at a pion CM angle of 90^{o}. The experimental technique required simultaneous detection of both the pions and the nucleons. Pions were detected by three scintillation counters. Lead plates of 2.4 radiation lengths and 1.2 radiation lengths were placed in front of the second and third counters. Neutral pions were identified by the absence of output in the first counter and the large outputs in the second and third counters. Nucleons were detected in two scintillation counters. The second of the two counters is 11" thick and has approximately 20% efficiency of detecting neutrons. Neutrons were identified by the absence of output in the first counter. The energy of the incident photons was determined by synchrotron subtraction. Since the statistical accuracy of synchrotron subtraction is poor, a system of three fast coincidence circuits was used as a time-of-flight instrument to reduce the number of events initiated by low energy photons. The statistical errors assigned to the ratio range between 15-30%.

The results of this experiment agree with the results of Bingham within statistical errors, but show a general tendency for the σ^{no}/σ^{o} ratio to be lower. The ratio of σ^{no}/σ^{o} obtained in this experiment ranges between 0.4 and 0.8. The cross sections for neutral pion photoproduction from neutrons are derived from the σ^{no}/σ^{o} ratio and the Caltech data on neutral pion photoproduction from hydrogen.

TABLE OF CONTENTS

APPENDICES

I. GENERAL CONSIDERATIONS

The existence of a "meson" was predicted by Yukawa in 1935 in his effort to explain the short-range and large-strength of nuclear forces. Such a particle, the pion, was discovered in 1947 in cosmic rays. Since then, a great deal of work has been done in the effort to understand the pion-nucleon interaction. Until recently, most of the work has been done on two simplest reactions, the pion-nucleon scattering and the photoproduction of pions.

Detailed measurements of the total cross sections and the differential cross sections for the photoproduction of positive pions and neutral pions from hydrogen have been made up to 1 Bev for the energy of the incident photons. The total cross section for photoproduction of positive pions increases from the threshold of 150 mev proportional to p, the momentum of pion in the CM system, rises to a maximum of 250 μb at approximately 320 mev. This is designated as the "first resonance". A "second resonance" is seen at approximately 750 mev with peak amplitude of 100 μb and a "third resonance" is seen at approximately 1050 mev. The total cross section for photoproduction of neutral pions rises from threshold proportional to p^3, reaches a peak of 270 μb at 320 mev and shows a maximum between 700-800 mev. The differential cross sections for the photoproduction of positive pions and neutral pions become more complex as the energy of the incident photons goes up.

Theoretically, low energy data up to 350 mev can be explained quite successfully by the static theory of Chew et al. (1) and more recently by the theory of Chew, Nambu et al. (2). However, at higher energies, no successful theory exists.

A phenomenological theory, based on the conservation laws of energy, momentum, isotopic spin, angular momentum and parity, can be used to analyze the data. The first resonance is dominated by the interaction of a state with isotopic spin $I = 3/2$, angular momentum $J = 3/2$ and even parity, thus a $p_{3/2}$ state. The second resonance is dominated by $I = 1/2$, $J = 3/2$ state, and odd parity, thus a $D_{3/2}$ state. The third resonance is not well known. At present, it is designated as $I = 1/2$, $J = 5/2$ state and even parity.

Since free neutrons are not available, the productions of negative pions and neutral pions from neutrons are much harder to measure. Deuterons, being the simplest nuclei, are generally used as the targets in experiments for the photoproductions of pions from neutrons. Unfortunately, complications arise when nuclei are used as targets. In addition to interactions of the photon and pion with a single target nucleon, one also has to take into account the interaction between the pion produced and the other nucleons, the interaction between the nucleons, and the interaction of the photon with other nucleons. Furthermore, in certain types of experiments which compare the yields from hydrogen and deuterium the results obtained may be difficult to interpret in terms of the photoproduction of pions from neutrons. From the point of view of an experimentalist, the motion of individual nucleons inside the deuteron nuclei smears out the kinematics and makes the determination of dynamical variables more difficult and less certain.

In spite of these difficulties, detailed measurements on the ratio of negative pions to positive pions from deuterons produced by photons have been carried out for photons from threshold energy up

to 1 Bev. (3) The total cross sections and differential cross sections of negative pions photoproduced from neutrons can be obtained from the π^-/π^+ ratio and the cross sections for π^+ production from hydrogen.

The measurement of neutral pions, produced from neutrons by photoproduction, is made even more difficult by the fact that both particles are neutral, and furthermore, the neutral pion decays rapidly into two photons. Tollestrup et al. (4) have measured the ratio of neutral pions produced from deuterium to that produced from hydrogen by photons of energies up to 400 mev at three laboratory angles, 30°, 73°, 140° by measuring the yields of the photons from the decayed neutral pion with a counter telescope. These measurements were extended to the range of 500-1000 mev by Bingham. (5)

The accuracy of Bingham's experiment is poor because it used the method of synchrotron subtraction to determine the energies of the incoming photons. The method of synchrotron subtraction involves the subtraction of data taken with the synchrotron set at a lower end point energy from that with synchrotron set at a higher end point energy with both sets of data properly normalized. The difference is due to photons of energies between the two end point energies.

Furthermore, the result obtained is the ratio of productions from deuterium to that from hydrogen. Its interpretation in terms of the neutral pion productions from protons and neutrons is uncertain.

In view of the above situation with respect to the neutral pion production from neutrons, this experiment was designed to measure directly the ratio of photoproduction of neutral pions from bound neutrons to that from bound protons in the energy range of 500-1000 mev with

better statistical accuracy than previously obtained. The experiment was performed in the hope that the knowledge of photoproduction of neutral pions from neutrons might help in our efforts to understand the pion-nucleon interaction.

II. INTRODUCTION TO THE EXPERIMENTAL TECHNIQUE

As mentioned before, the purpose of this experiment is to measure the cross sections of photoproduction of neutral pions from neutrons. Because of the absence of free neutrons in our world, the experiment must be done with some complex nuclei as targets. Deuterons, being the simplest nuclei, each containing one proton and one neutron loosely bound, are generally used. In the effort to ease the task of detecting the neutral particles and determining the counting efficiencies for the neutral particles, two methods are possible for this experiment. In the first method, one avoids the problem of detecting the neutrons. The neutral pions produced from both protons and neutrons in deuterons are detected. These data, properly normalized, are compared to the data obtained with hydrogen as target. Thus a ratio of π^{o} produced from D_2 to π^{o} produced from H_2 can be obtained. From this ratio, one hopes to deduce a ratio for π^{o} produced from free neutrons to π^{o} produced from free protons. This method obviously has certain defects. Theoretically, it is hard to deduce a ratio for π^{o} produced from free neutrons to π^{o} produced from free protons due to complications arising when deuterons are used as targets as mentioned before. Experimentally, the analysis involved in determining what fraction of photons comes from π^{o} of single pion production and what fraction from π^{o} of double pion production is always difficult. Still, this method has been used by Bingham (5) with some success.

The second method was suggested by R. L. Walker and is used in this experiment. It is designed to measure the ratio of π^{o} produced in protons and neutrons in deuterium by observing both the

nucleons and pions from the following reactions

1) $\gamma + n \rightarrow n + \pi^o$

2) $\gamma + p \rightarrow p + \pi^o$

3) $\gamma + p \rightarrow n + \pi^+$

4) $\gamma + n \rightarrow p + \pi^-$

Theoretically, the ratio of π^o produced from bound neutrons to that from bound protons is more satisfactory than the ratio obtained by the first method in deducing the cross section of photoproduction of π^o from free neutrons. The strong interaction between nucleons are now the same for reactions (1) and (2). The Pauli exclusion principle is also the same for both reactions. The Coulomb correction does not affect the production of neutral pions.

Experimentally, since the counting rates of reactions (3) and (4) are measured at the same time, the efficiency of counting neutrons can be calibrated by the known values of the σ^-/σ^+ ratio. This will now be explained in detail.

Let

σ^{no} be the cross section of reaction (1)

σ^o be the cross section of reaction (2)

σ^+ be the cross section of reaction (3)

σ^- be the cross section of reaction (4)

C^{no} be the counting rate of reaction (1)

C^o be the counting rate of reaction (2)

C^+ be the counting rate of reaction (3)

C^- be the counting rate of reaction (4)

ρ^{o} efficiency for the pion counter to count neutral pions

$\rho^{\pm}$ efficiency for the pion counter to count charged pions

ρ^{p} efficiency for the nucleon counter to count protons

ρ^{n} efficiency for the nucleon counter to count neutrons

$\eta^{no}(k)$ efficiency of the electronics to count reaction (1) determined by the resolution of the fast coincidence circuits system

$\eta^{o}(k)$ efficiency of the electronics to count reaction (2)

$\eta^{+}(k)$ efficiency of the electronics to count reaction (3)

$\eta^{-}(k)$ efficiency of the electronics to count reaction (4)

$\zeta^{o}(E_{\pi})$ the geometric efficiency for counting π^{o} due to the angular spreading of the γ-rays from decayed π^{o}, and E_{π} is the energy of the pion in the laboratory system

K energy of the photon in the nucleon rest system

k energy of the photon in the laboratory system

E_{o} synchrotron end point energy

W the total energy per BIP where BIP is a unit of energy used in our synchrotron laboratory

$\frac{W}{E_{o}} \frac{b(k/E_{o})}{k} = n(k)dk$ the number of photons per BIP of energy k within energy interval dk and $b(k/E_{o})$ is a function which describes the shape of the bremsstrahlung spectrum and satisfies the relation $\int_{o}^{1} b(k/E_{o})d(k/E_{o}) = 1$

N the number of target nucleons per cm^2 in the laboratory system

$\sigma(\theta')$ the differential cross section in the CM system

$d\Omega_N$ the solid angle for detecting nucleons in the laboratory system

$\frac{d\Omega'_N}{d\Omega_N}$ the solid angle transformation from the CM system to the laboratory system

$h(P_T)\frac{dP_T d\Omega_T}{4\pi}$ the probability, normalized to unity, of a target nucleon having a momentum P_T at angle θ_T, ϕ_T with solid angle $d\Omega_T$

$\epsilon(\theta_\pi)$ a function equal to 1 if pion is emitted within the angular range of the pion counters, 0, if not, and θ_π is the laboratory angle of the pion.

We can write down the following four equations

$$C^{no} = \frac{NW}{E_o}\int_{\underline{P}_T}\int_K \sigma^{no}(\theta')\frac{d\Omega'_N}{d\Omega_N}\frac{b(k/E_o)}{k}\Delta\Omega_N \rho^o\zeta^o(E_\pi)\rho^n\eta^{no}(k)\epsilon(\theta_\pi)h(P_T)dP_T\frac{d\Omega_T}{4\pi}dK^*$$

$$= A\,\overline{\sigma^{no}(\theta')}\;\rho^o\zeta^o(E_\pi)\rho^n\eta^{no}(k) \qquad (5)$$

$$C^o = \frac{NW}{E_o}\int_{\underline{P}_T}\int_K \sigma^o(\theta')\frac{d\Omega'_N}{d\Omega_N}\frac{b(k/E_o)}{k}\Delta\Omega_N \rho^o\zeta^o(E_\pi)\rho^p\eta^o(k)\epsilon(\theta_\pi)h(P_T)dP_T\frac{d\Omega_T}{4\pi}dK$$

$$= A\,\overline{\sigma^o(\theta')}\;\rho^o\zeta^o(E_\pi)\rho^p\eta^o(k) \qquad (6)$$

---

*For derivation of this expression, see derivation of a similar expression in Neugebauer's thesis.

$$C^{+} \equiv \frac{NW}{E_o} \int_{\underline{P}_T} \int_K \sigma^{+}(\theta^{\prime}) \frac{d\Omega^{\prime}{}_N}{d\Omega_N} \frac{b(k/E_o)}{k} \Delta\Omega_N \rho^{+}_{-} \rho^{n} \eta^{+}(k) \epsilon(\theta_\pi) h(P_T) dP_T \frac{d\Omega_T}{4\pi} dK$$

$$\equiv A \overline{\sigma^{+}(\theta^{\prime})} \rho^{+}_{-} \rho^{n} \eta^{+}(k) \tag{7}$$

$$C^{-} \equiv \frac{NW}{E_o} \int_{\underline{P}_T} \int_K \sigma^{-}(\theta^{\prime}) \frac{d\Omega^{\prime}{}_N}{d\Omega_N} \frac{b(k/E_o)}{k} \Delta\Omega_N \rho^{+}_{-} \rho^{p} \eta^{-}(k) \epsilon(\theta_\pi) h(P_T) dP_T \frac{d\Omega_T}{4\pi} dK$$

$$\equiv A \overline{\sigma^{-}(\theta^{\prime})} \rho^{+}_{-} \rho^{p} \eta^{-}(k) \tag{8}$$

where $A \equiv \int_{\underline{P}_T} \int_K \frac{NW}{E_o} \frac{d\Omega^{\prime}{}_N}{d\Omega_N} \Delta\Omega_N dK h(P_T) \underline{dP_T} \frac{d\Omega_T}{4\pi} \epsilon(\theta_\pi)$ is a constant and the same for all four reactions, and $\sigma(\theta^{\prime})$ is the average cross section within the energy interval. Then from (5) and (6)

$$\frac{\sigma^{no}}{\sigma^{o}} \equiv \frac{C^{no}}{C^{o}} \frac{\rho^{p}}{\rho^{n}} \frac{\eta^{o}}{\eta^{on}}$$

from (7) and (8)

$$\frac{\rho^{p}}{p^{n}} \equiv \frac{C^{-}}{C^{+}} \frac{\eta^{-}}{\eta^{+}} \frac{\sigma^{+}}{\sigma^{-}}$$

Thus

$$\frac{\sigma^{no}}{\sigma^{o}} \equiv \frac{C^{no}}{C^{o}} \frac{C^{-}}{C^{+}} \left(\frac{\eta^{o}\eta^{-}}{\eta^{no}\eta^{+}}\right) \frac{\sigma^{+}}{\sigma^{-}}$$

Now all counter efficiencies have been eliminated and if the electronic system counts all four reactions with equal efficiency which will be verified later, then the above equation reduces into the following simple one

$$\frac{\sigma^{no}}{\sigma^{o}} = \frac{C^{no}}{C^{o}} \frac{C^{-}}{C^{+}} \frac{\sigma^{+}}{\sigma^{-}}$$

For this experiment, a set of two counters was used to detect the nucleons and a set of three counters was used to detect the pions. In principle, the energy of the photon can be inferred from the energy of the nucleon whose time-of-flight with respect to the pion was measured by a set of three coincidence circuits. Due to a) the relatively high speed of the nucleons b) the smearing effect due to the internal motion of the nucleons in the deuteron and c) the difficulty in making fast coincidence circuits work with resolution of less than 5 nanoseconds and variations of amplitude of 300% in input pulses, a synchrotron subtraction was necessary in order to obtain a reasonable energy resolution as in the experiment of Bingham. The fast coincidence circuit system was used only to cut out events initiated by photons of very low energies, and thus to improve the statistical accuracy of the synchrotron subtraction method.

The pulses from the five counters used in this experiment were recorded on film and the four relevant reactions were identified by pulse height analysis. The details of this analysis will be explained in Section V.

Since all the counter efficiencies cancel out, the requirements for identification of a particular reaction were set very stringent to avoid any wrong identification. Thus, events which showed the slightest ambiguity in their identification were thrown out. Any wrong identification will introduce a correction to our final results. Estimates of these corrections are shown in Appendix IV. The corrections are very small and are not included in our final results.

III. EQUIPMENT

The experimental area of the Caltech synchrotron is shown in Figure 1.

A. Synchrotron

The bremsstrahlung beam of the Caltech synchrotron is produced once a second for a 40 millisecond "dump" during which the electron energy is held constant. The energy, called E_o, is measured by a beam energy meter which measures the magnetic field during the dump time of the synchrotron. The accuracy to which E_o is determined is limited by systematic errors which can be as large as one percent. In this experiment, E_o was set at 700, 800, 950 and 1150 mev at various times.

The beam is collimated by a series of lead apertures to form a rectangular beam. The data for the points $\theta'_\pi = 60^o$, where θ'_π is the CM angle of the pion, were taken with the target very close to the synchrotron. The size of the beam at the target measured 7/8" x 1 1/8". The data for $\theta'_\pi = 90^o$ were taken with the target approximately four feet further away from the synchrotron where the size of the beam was 1 1/8" x 1 3/8". This change was made in order to allow other experiments to run concurrently.

Two different ionization chambers were used to monitor the energy in the beam. For the first part of this experiment, including data for points 1, 2, and part of 3, a Cornell type thick-walled ionization chamber (Chamber A) was used. For the second part of this experiment, another ionization chamber of the same type was used. Both chambers have been calibrated against the Cornell

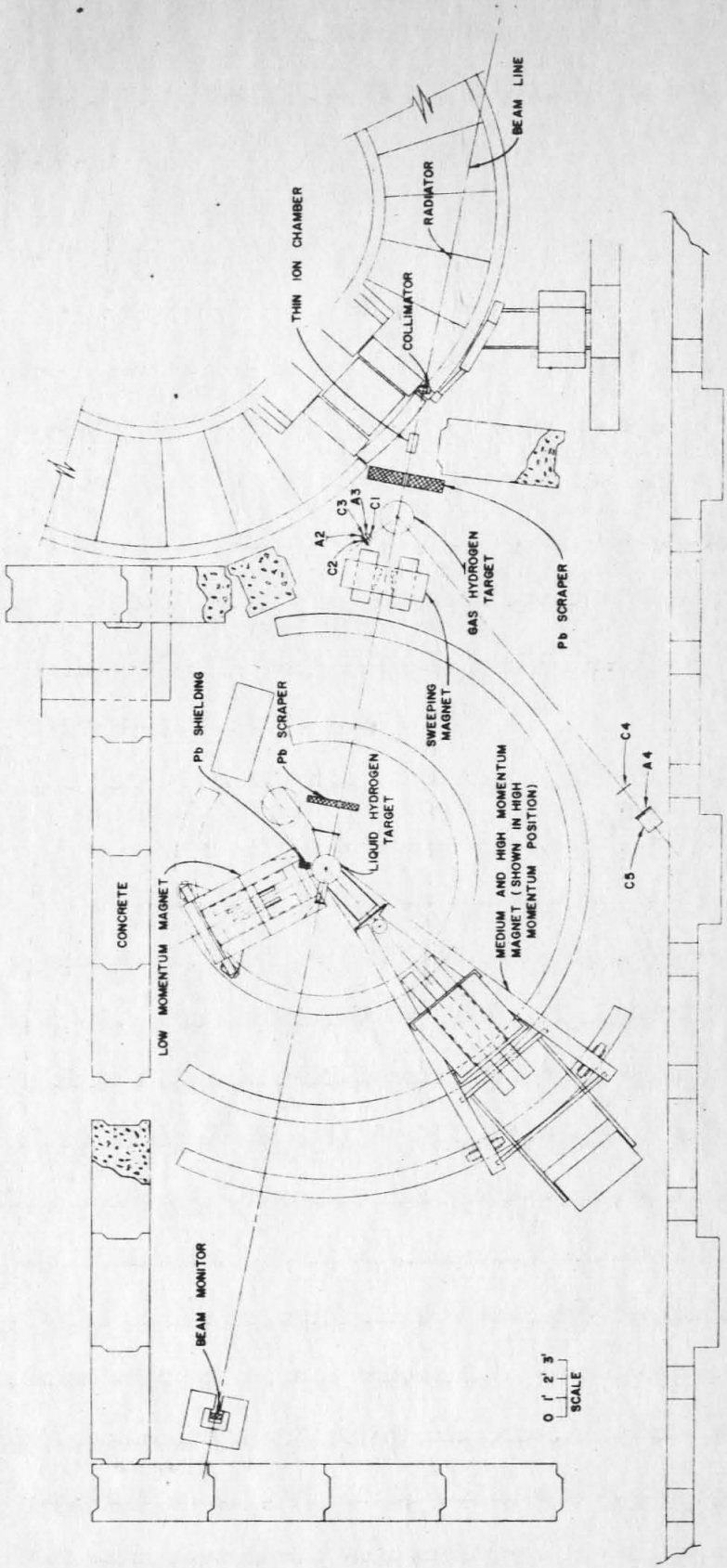

Synchrotron Experimental Area

Figure 1

Quantameter. The integrated beam energy was measured in units of BIPS- Beam Integrator Pulses. The energy per BIP depended on the chamber and varied linearly with E_o. Table 1 shows the variation. A typical synchrotron beam intensity was 5 BIPS per minute; however large variations occurred.

The energy spectrum of the photons is given by

$$n(k)dk = \frac{W}{E_o}\, b(k/E_o)\, \frac{dk}{k}$$

where n(k)dk is the number of photons per BIP of energy k within an energy interval dk, W is the total energy in the beam per BIP and $b(k/E_o)$ is a function such that

$$\int_o^1 b(k/E_o)\, d(k/E_o) = 1 .$$

The function $b(k/E_o)$ has been measured by J. Boyden. (6) It is shown in Figure 2.

B. Target

The target used was deuterium gas at high pressure contained in a nickel-coated steel cylinder with hemispheric ends. The cylinder was 2 inches in diameter and 17 inches long for the straight part. In order to reduce background, the target was shielded in such a way so that only the middle portion of the target was seen by the counters. The target was emptied when data were not being taken. A liquid nitrogen reservoir, located on top of the target, was used to cool the target. Pressure was given by a pressure gauge, the error in reading being about 0.5% . The temperature was given by an iron-constantan thermocouple on the outer surface of the target near the

Table 1

Ion Chamber Calibrations

Chamber A

Energy (mev)	Chamber Sens. U $\frac{10^{18}\ \text{mev}}{\text{coul}}$	Integrator Cal. M $\frac{10^{-6}\ \text{coul}}{\text{BIP}}$	Energy per BIP W = UM $\frac{10^{12}\ \text{mev}}{\text{BIP}}$	Equivalent quanta* per BIP $\frac{UM}{E}$
700	4.41	0.211	0.931	1.33
800	4.36	0.211	0.921	1.15
950	4.29	0.211	0.906	0.954
1150	4.20	0.211	0.886	0.770

Chamber B

Energy (mev)	U $\frac{10^{18}\ \text{mev}}{\text{coul}}$	M $\frac{10^{-6}\ \text{coul}}{\text{BIP}}$	UM $\frac{10^{12}\ \text{mev}}{\text{BIP}}$	$\frac{UM}{E}$
700	4.87	0.211	1.03	1.47
800	5.09	0.211	1.07	1.34
950	5.38	0.211	1.13	1.19
1150	5.66	0.211	1.19	1.04

$M = 0.211 \times 10^{-6}$ coul/BIP is the calibration of the integrator.

U, the energy per coulomb, is a property of the chamber.

---

*Equivalent quanta is defined in Section VI.

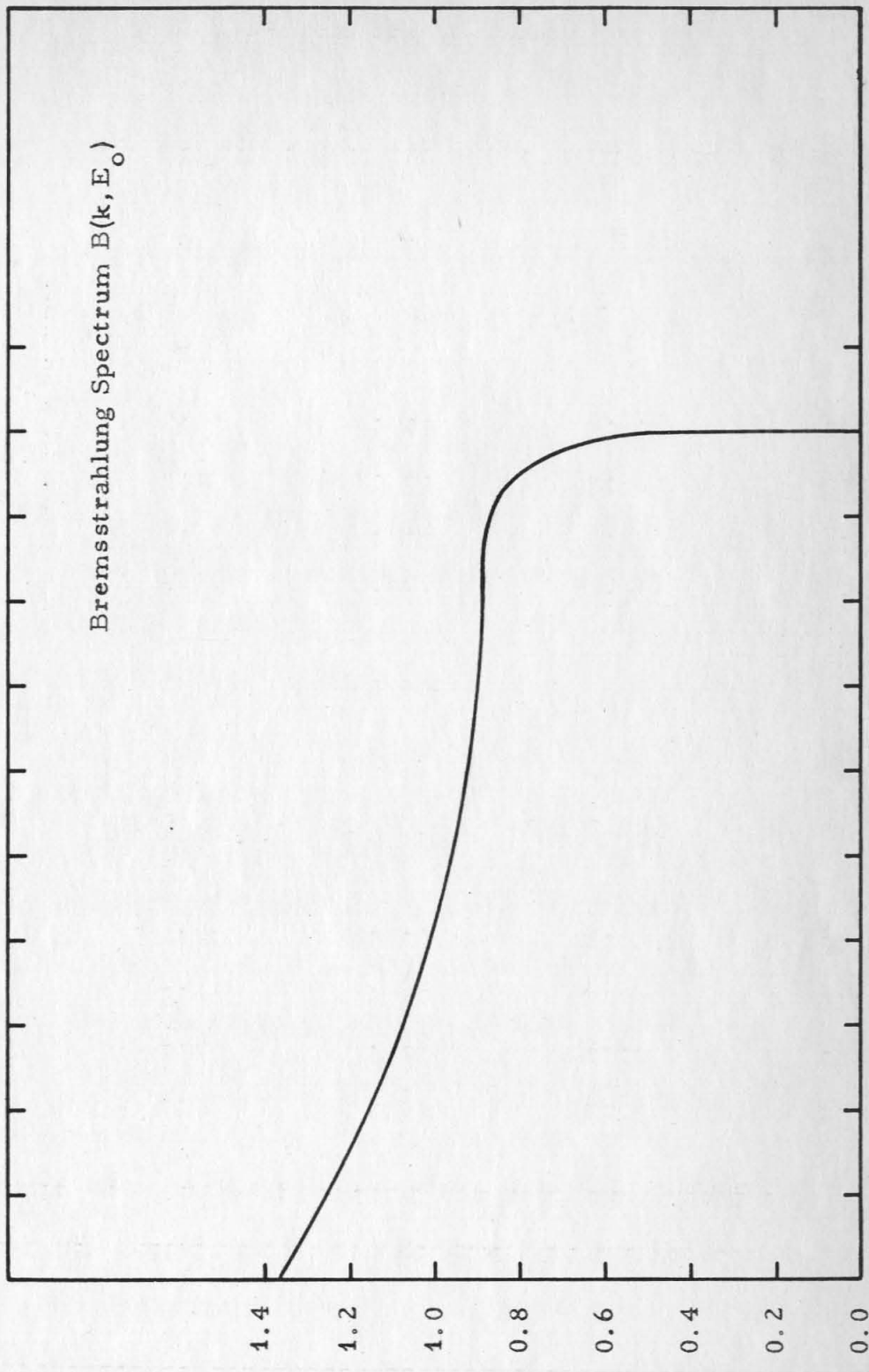
Bremsstrahlung Spectrum B(k,E$_o$)
1.4
1.2
1.0
0.8
0.6
0.4
0.2
0.0
0.1 0.2 0.3 0.4 0.5 0.6 0.7 0.8 0.9 1.0 1.1
k/E$_o$

Figure 2

front end. A reference temperature was provided by another thermocouple immersed in liquid nitrogen. The temperature could be measured to about 0.5% . The density was found from temperature and pressure measurement by interpolation from data of Johnson et al. (7) The absolute error in the density measurement was about 3%. The relative error from run to run was about 1% . The target is shown in Figure 3.

C. Counters

A diagram of the counters is shown in Figure 4. Pions were detected by a set of three scintillation counters C1, C2, and C3. The sizes of these counters and the spacings between them are shown in Table 2. The distance from the target to the front surface of C3, determined by the compromise between high counting rates in the counters which give high accidental rates and maximum efficiency in accepting the photons from the decay of neutral pions, was 24 inches for $\theta'_\pi = 60^\circ$ and 20 inches for $\theta'_\pi = 90^\circ$. Pulse heights for charged pions were proportional to the specific ionization dE/dx, and the charged pions in question were minimum ionizing particles.

C1 was also used as a veto counter for neutral pions. A piece of lead 1/2 inch thick was put in front of C2 and another piece 1/4 inch thick, in front of C3. These lead pieces were used to convert the photons from decayed neutral pions into showers to give large pulses in C2 and C3. The thicknesses of the lead plates, corresponding to 2.4 radiation lengths and 1.2 radiation lengths respectively, were chosen to give approximately the maximum number of secondary electrons for photons from the decay of π° produced in this experiment,

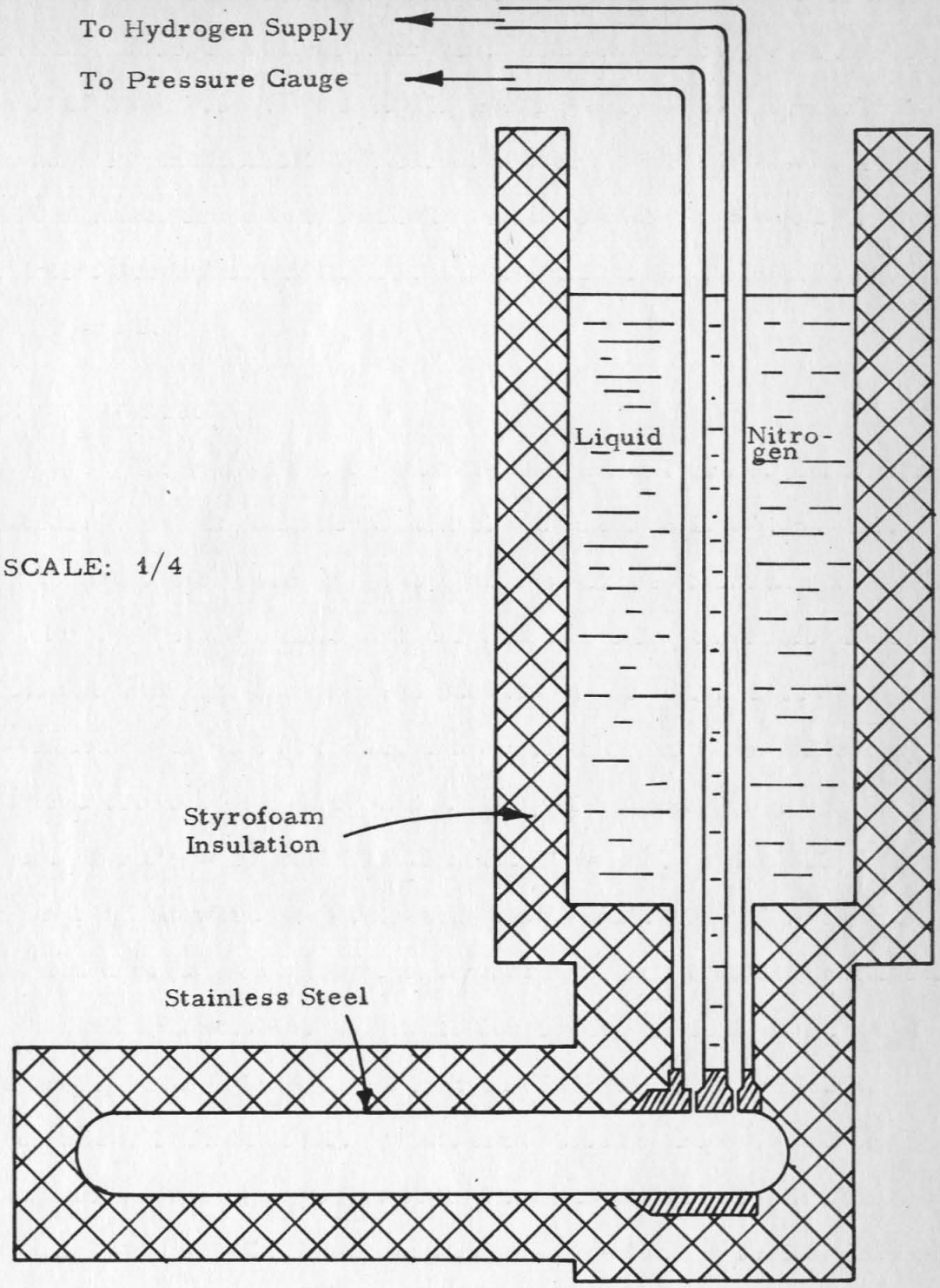

Gas Target

Figure 3

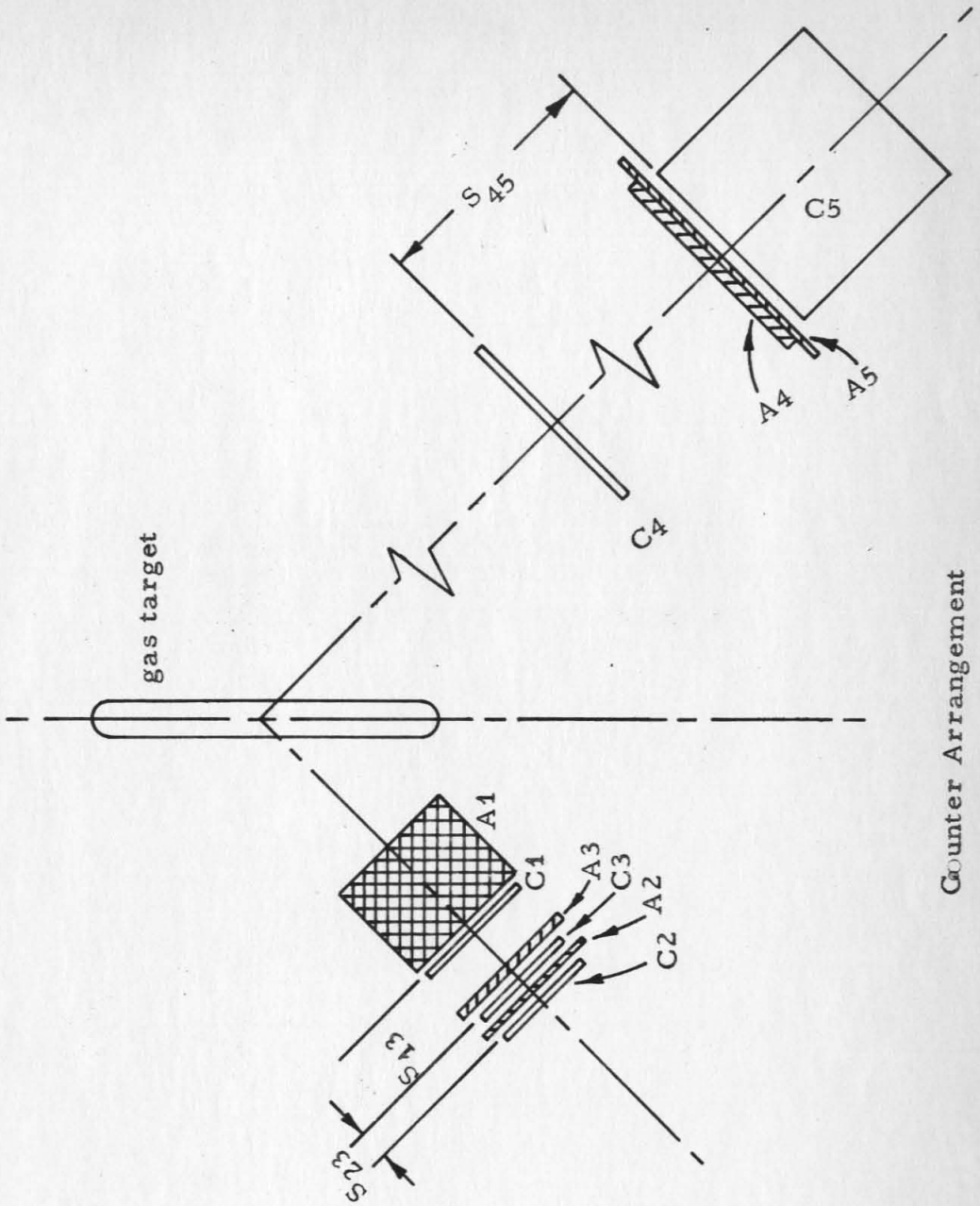

Counter Arrangement

Figure 4

Table 2

Dimensions of Counters and Absorbers, and Distances

Counters	Absorbers	Distances
C1 9" x 7" x $\frac{1}{2}$"	A1 parafin 6"	$S_{13} = 3\frac{1}{2}$"
C2 7" x $6\frac{1}{4}$" x $\frac{1}{2}$"	A2 lead $\frac{1}{4}$"	$S_{23} = 1\frac{1}{2}$"
C3 8" x $6\frac{1}{2}$" x $\frac{1}{2}$"	A3 lead $\frac{1}{2}$"	$S_{45} = 20$"
C4 22" x 11" x $\frac{1}{4}$"	A4 lead $\frac{1}{2}$"	
C5 22" x 11" x 11"	A5 aluminum $\frac{1}{4}$"	

as shown by Wilson. (8) The reason that two pieces of lead were used instead of one piece of thickness equal to the sum of the thicknesses of the two pieces was to insure that pulse heights from C2 and C3 were independent to each other. The geometric efficiency of seeing a photon from the decay of a neutral pion was determined by C2. This efficiency varied from 40% to 80% depending on the energy and angle of the neutral pion. The absolute value of this efficiency is not important in this experiment as has been shown before.

Four pieces of paraffin totaling 6 inches thick, corresponding approximately to 0.3 radiation length, were placed in front of the counters to cut down the single counting rates in the counters. Any event with the photon from neutral pion decay initiating a shower in paraffin and giving a pulse in C1, was thrown out in the final analysis. This is possible because the precise knowledge of this efficiency is not important for the experiment as in the case of geometric efficiency; likewise, the precise knowledge of the effect of absorption of charged pions by paraffin and lead is not important for this experiment if the effects of π^+ and π^- are equal. Neugebauer and Wales (9) have shown in their experiment the absorption corrections of π^+ and π^- are equal.

Each counter was viewed by a single 6810 RCA phototube.

Nucleons were detected by two scintillation counters designed by Dr. K. Althoff. Their dimensions and constructions are shown in Figure 5. The distance from the target to C4, determined by the physical dimensions of our laboratory and the time-of-flight desired, was 5.4 meters for $\theta'_\pi = 60^\circ$ and 7.1 meters for $\theta'_\pi = 90^\circ$. Counter 4 was used to distinguish protons from neutrons. It was made of a 1/4 inch

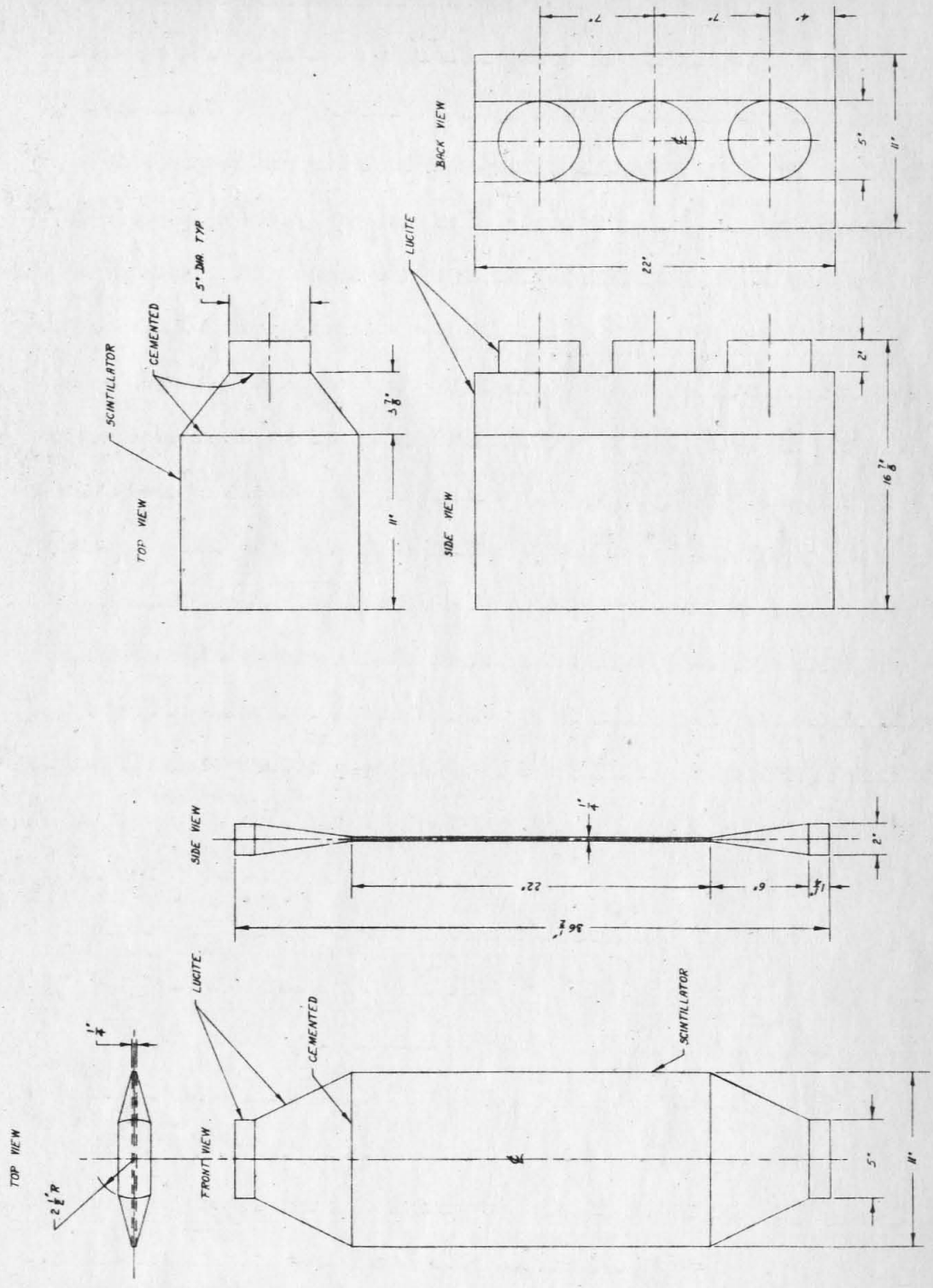
TOP VIEW
SCINTILLATOR
CEMENTED
5" DIA TYP
SIDE VIEW
LUCITE
BACK VIEW
22"
11"
5"
2"
Counter 5
TOP VIEW
FRONT VIEW
LUCITE
CEMENTED
SCINTILLATOR
SIDE VIEW
22"
2"
5"
11"
Counter 4

Figure 5

thick sheet of plastic scintillator in order to reduce the probability of converting neutrons as much as possible without sacrificing the efficiency of counting protons. It was viewed by two 7046 RCA phototubes.

Counter 5 determined the aperture of this experiment. Table 3 shows the geometric apertures of the data points. The signal of C5, together with those of counter 2 and counter 3, were fed into a system of three coincidence circuits. The output of the coincidence circuit system was used as a trigger for an event. The counter C5 was made of a plastic scintillator block 22" x 11" x 11". Neutrons have approximately 20% probability of being converted. (10) It was viewed by three 7046 RCA photomultiplier tubes.

A piece of lead 1/2 inch thick was put in front of counter 5 for data points 1, 2, and 3a in an attempt to increase the efficiency of counting neutrons.

D. Electronics

A block diagram of the electronics is shown in Figure 6.

The signals from C2 and C3 were divided by two resistance networks. 75% of each signal went into a delay and mixer. 25% went into a 460A Hewlett-Packard amplifier which had an amplification factor of 3. The outputs of the two amplifiers were fed into two primary fast coincidence circuits which had 5 nanoseconds clipping stubs.

The signals of the three phototubes of C5 were added together at the bases of these phototubes by adjusting the voltages on grid 1 and dynode 1 of these phototubes to compensate the inherent difference

Table 3

Experimental Conditions for the Data Points

Point	θ_N	D_N	θ_π	D_π	E_{01} (mev)	E_{02} (mev)	T (ns)	Solid angle (sr.)
1	50.3°	5.4M	42°	.61M	1150	950	27.4	.0053
2	50.3°	5.4M	42°	.61M	950	800	31.4	.0053
3	50.3°	5.4M	42°	.61M	800	700	35.4	.0053
4	39.8°	7.1M	60°	.51M	1150	950	32.5	.0031
5	39.8°	7.1M	60°	.51M	950	800	32.5	.0031

θ_N Lab angle of the nucleon counters

θ_π Lab angle of the pion counters

D_N Distance from target to center of C5

D_π Distance from target to C3

E_{01} Upper end point energy of the synchrotron beam

E_{02} Lower end point energy of the synchrotron beam

T Delay on C5 with respect to C2 and C3

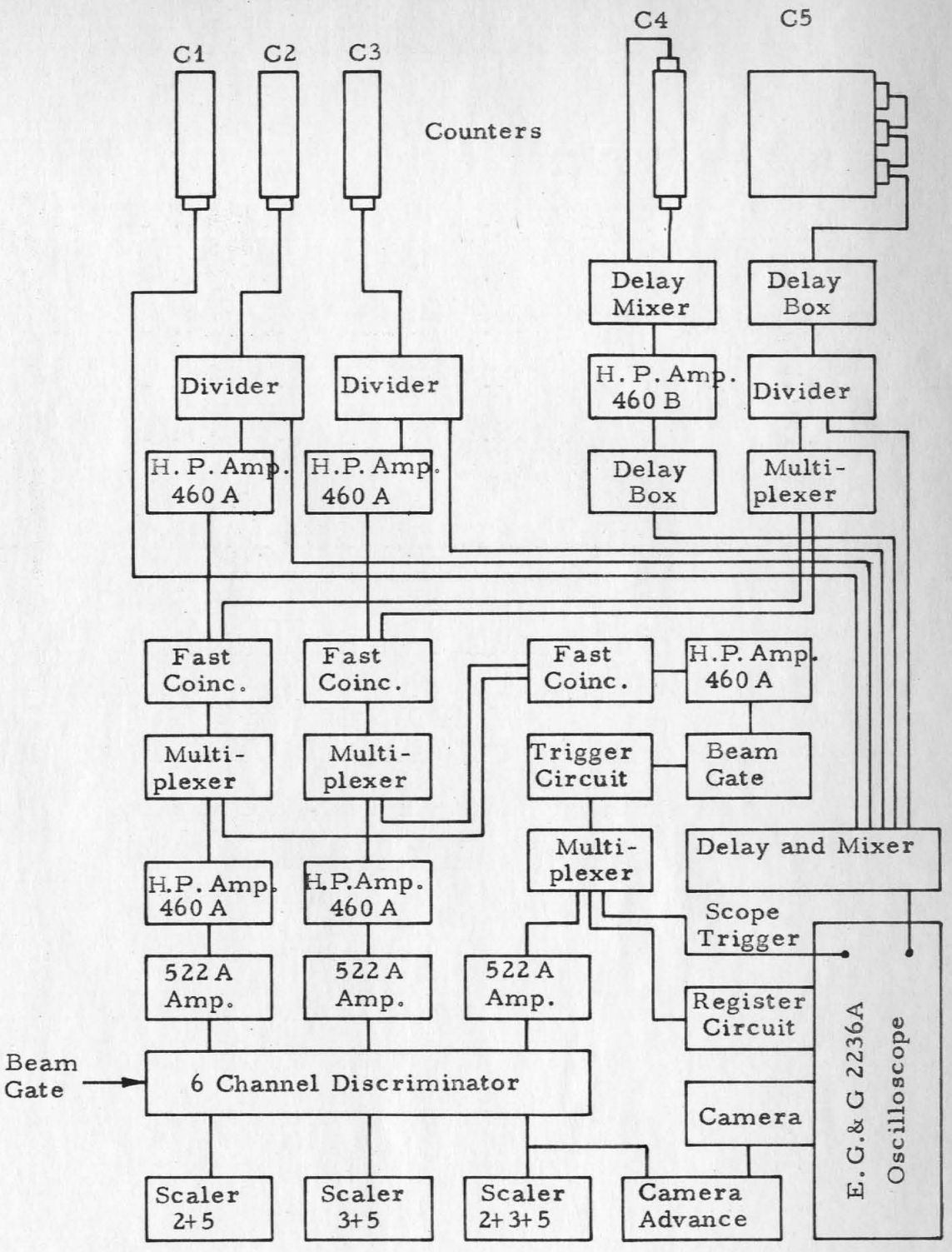

Electronic Block Diagram

Figure 6

in transit time of these phototubes which might be as large as 5 nanoseconds. The resultant signal was then divided in the same manner as for C2 and C3. 75% of the signal went into a delay and mixer, 25% of the signal went into a 3-channel multiplexer which gave three outputs of equal amplitudes as the input signal. Two outputs of this multiplexer went into the fast coincidence circuits mentioned above.

The output of each of these two fast coincidence circuits first went into a multiplexer. The outputs of the multiplexers then went into a secondary fast coincidence circuit which had a theoretical resolution of 25 nanoseconds. Due to the high counting rates in C2 and C3, two primary fast coincidence circuits were used instead of one, in order to cut down the number of accidentals. The function of the secondary coincidence circuit was to insure that the signals from counter 2 and counter 3 were truly in coincidence.

One of the outputs of the multiplexers for the primary coincidence circuits, after proper amplification by a HP 460 A amplifier and a 522 A amplifier, was fed into a gated 6-channel discriminator. The output of the discriminator then energized a scaler. The gate on the discriminator was centered on the beam dump.

The output of the secondary coincidence circuit, after being amplified by a HP 460 A and passing through a gate which was centered on the beam dump, was fed into a biased trigger circuit which gave a standard output pulse of 10 volts, 50 nanoseconds long. The output of the trigger circuit went into a multiplexer. One output of the multiplexer was used to trigger the oscilloscope, and one to trigger the "register" circuit. The function of the "register" circuit was to put a number on the film for each event. The other output of the

multiplexer, after being amplified by a 522 A amplifier, was divided into two parts, one being used to advance the camera, and the other going into the 6-channel discriminator whose output energized a scaler.

The signals for the two phototubes of counter 4 were added together in a delay and mixer. The signals could not be added in the same manner as C5 because the two phototubes were physically separated by 6 nanoseconds and the adjustment of voltage on grid 1 and dynode 1 could not compensate so much time difference. The resultant signal was then amplified by a HP 460 B amplifier and fed into the same delay and mixer as signals from C2, C3, and C5.

The signals from C1 were fed directly into the delay and mixer.

The output of the delay and mixer was fed into a EG&G Type 2366A oscilloscope.

IV. PROCEDURE

In this section, the experimental procedure for obtaining the data is described.

A) Energy Resolution

As was mentioned before, the time-of-flight technique does not work very well for this experiment. Because of the physical limitations of our laboratory, the difference in time for a nucleon produced at laboratory angle of 50° by a photon of 1000 mev and a photon of 800 mev to travel from the target to C5 differs only by 2.5 nanoseconds. For a fast coincidence circuit to work with resolution of this order of magnitude, requires that the amplitudes of the input pulses have very small dispersion--a condition which is not valid in this experiment since the pulse amplitude of a neutral pion may be four times as large as the pulse amplitude of a charged pion.

Thus the energy resolution in this experiment was determined by synchrotron subtraction. Two sets of data were taken, one with synchrotron end point energy set at a value higher by a desired value than the other (see Table 3). The difference of the two sets of data, when each was properly normalized, represented the contributions due to photons of energies between the two values of the end point energies. Because of the large angle the pion counters sustained toward the target, almost all energies above the single pion production threshold in the bremsstrahlung spectrum could produce an event with detectable pion and nucleon. Hence the statistics of synchrotron subtraction was bad if the difference in end-point energies was small compared to the energies themselves. In order to improve statistics, fast coincidence circuits with resolution of 5 nanoseconds

were used to reduce the number of events produced by low energy photons. As mentioned before, the output of the coincidence circuit system also served the important function as a trigger for an event.

The resolution of these three coincidence circuits, with actual phototube pulses as inputs, was measured in the following manner. Counters 2 and 3 were placed directly in front of counter 5. Particles produced by the synchrotron beam striking a target passed through all three counters simultaneously. The signals from these counters were fed into the coincidence circuits. By introducing artificial delay in signals of counter 5, a resolution curve was obtained as shown in Figure 7. To measure the efficiency of the fast coincidence circuit system, a small counter C_s, 4" x 4" x 1/2", was placed in front of the three counters. The output of this counter was put in fast coincidence with counter 5. The output of this coincidence was put in slow coincidence with the output of the fast coincidence system of C2, C3, and C5. The efficiency was calculated from the following expression.

$$\text{efficiency} = \frac{(C_s \cdot C5) \cdot (C2 \cdot C3 \cdot C5)}{(C_s \cdot C5)}$$

The flat top of this resolution curve indicates that the efficiency of this system is nearly 100%. The deviation of the absolute value of the efficiency from 100% was probably due to the inefficiencies of individual counters.

The delay of C5 with respect to C2 and C3 for all experimental points except point 5 was so adjusted that the data obtained from synchrotron subtraction consisted of events accepted within the flat part

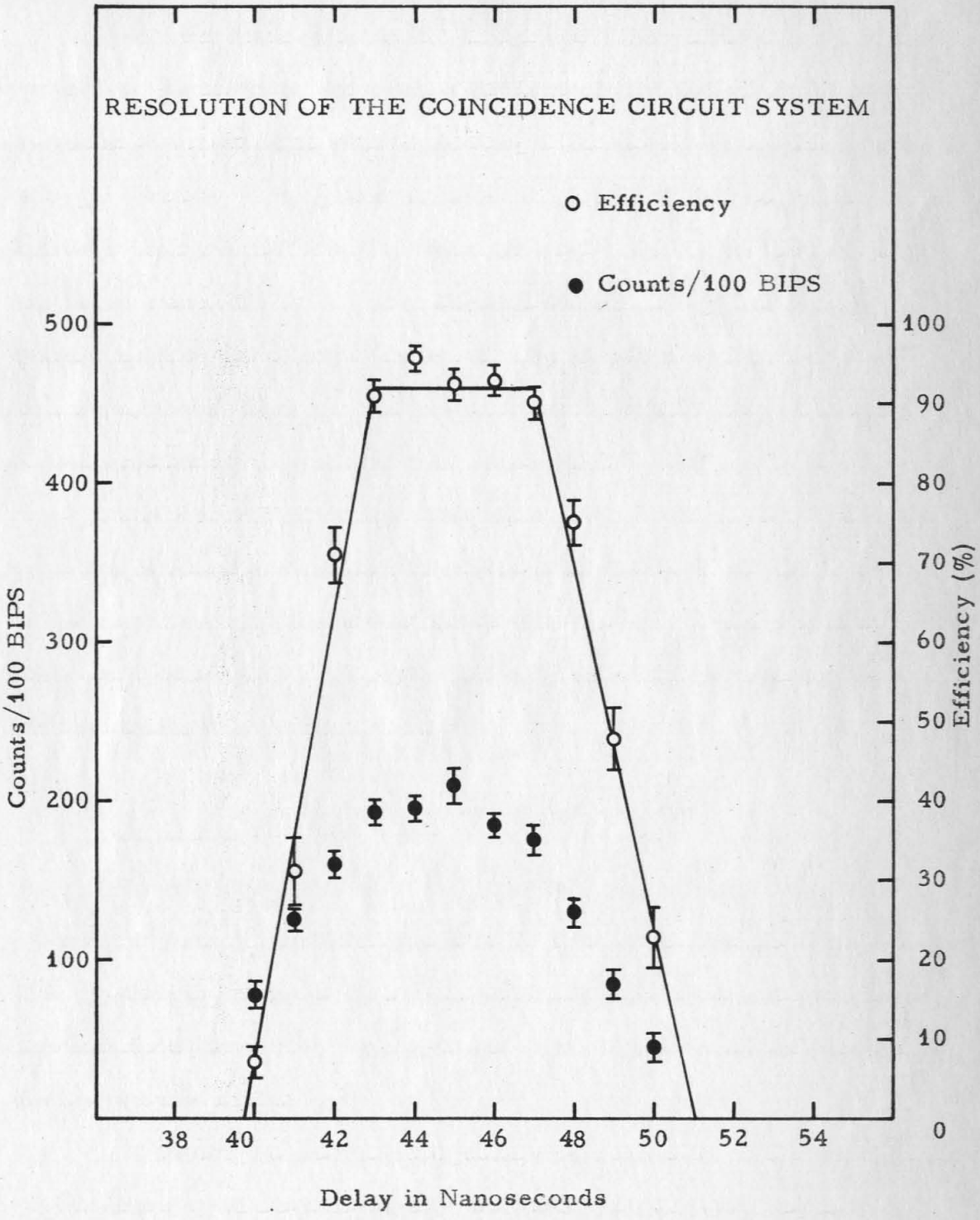
RESOLUTION OF THE COINCIDENCE CIRCUIT SYSTEM
Efficiency
Counts/100 BIPS
Counts/100 BIPS
Efficiency (%)
Delay in Nanoseconds
500
400
300
200
100
100
90
80
70
60
50
40
30
20
10
0
38
40
42
44
46
48
50
52
54

Figure 7

of the coincidence circuits resolution to insure equal counting efficiencies (100%) for all four reactions.

The expression for the resolution of the electronic circuit system as a function of photon energy with hydrogen as the target is similar to the expression for deuterium shown in Section II except for the factors which take account of the internal motion of the nucleons in the deuteron. An example of this resolution function is shown as Curve A in Figure 8. This curve was calculated from the solid curve in Figure 6 by assuming that the protons came out at laboratory angles of 50.3° and had a time-of-flight path length of 5.4 meters and that the time delay on the coincidence circuits was set so that protons produced at this angle by 760 mev photons would be too slow to be in coincidence with the pions.

When D_2 was used as target, the internal motion of the nucleons in the deuterons smeared out the resolution curve. A calculation similar to the one made by Neugebauer and Wales (9) using spectator model for deuteron was carried out, and the resulting resolution curve is shown as Curve B in Figure 8. The details of the calculation are shown in Section V.

It was also obvious from the curve that in order to obtain a reasonable energy resolution for this experiment, a synchrotron subtraction was necessary as mentioned before. The subtraction could not be arbitrarily narrow; it must be compromised by the statistical accuracy one wishes to obtain in a reasonable amount of time for the experiment. The widths of the energy resolution for the data points are shown in Table 3. The counting rates at the upper synchrotron end point energies were approximately twice those at the lower end point energies for all experimental points when both counting rates were properly normalized.

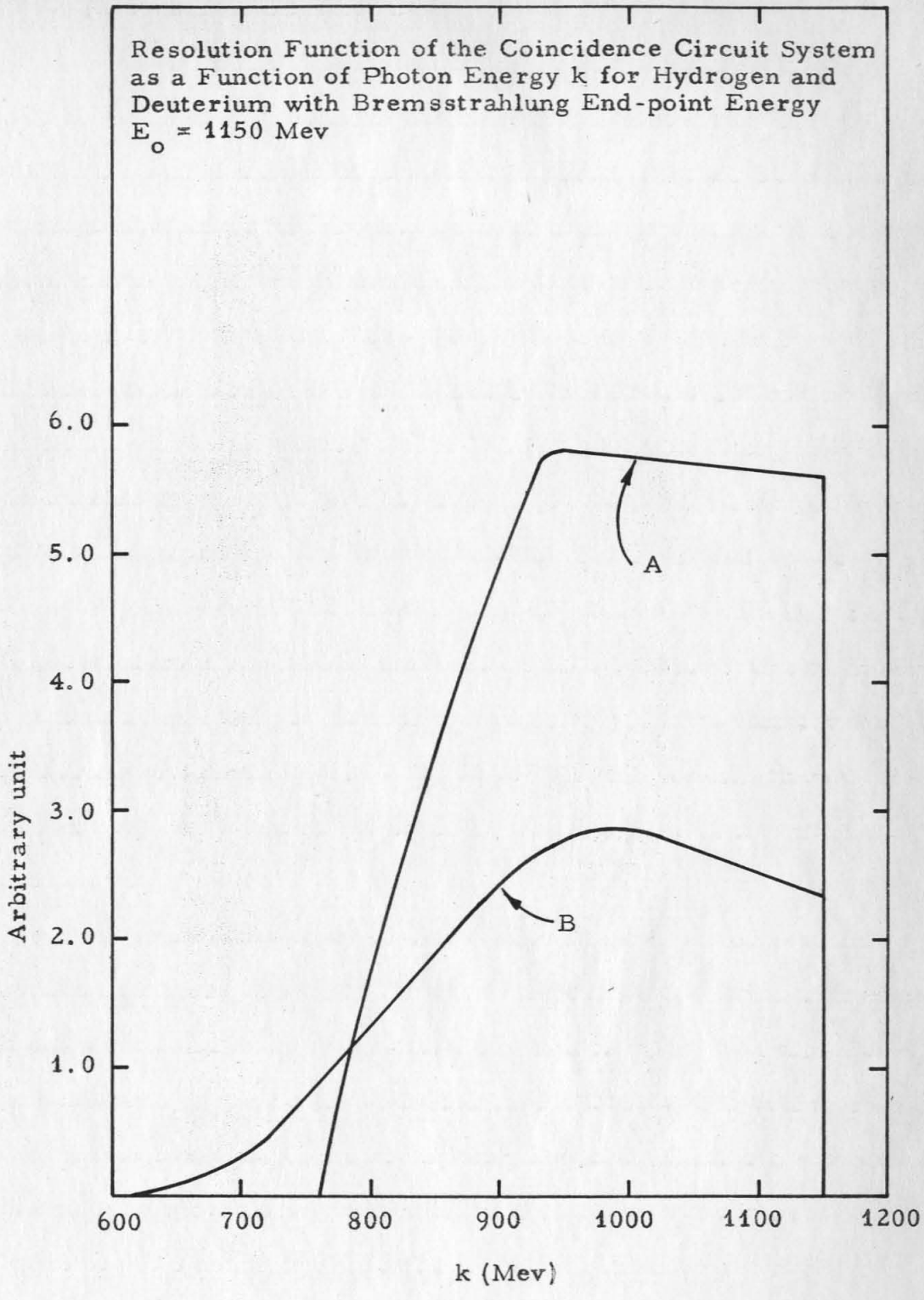
Resolution Function of the Coincidence Circuit System as a Function of Photon Energy k for Hydrogen and Deuterium with Bremsstrahlung End-point Energy E_o = 1150 Mev
Arbitrary unit
6.0
5.0
4.0
3.0
2.0
1.0
A
B
600
700
800
900
1000
1100
1200
k (Mev)

Figure 8

B) Data Recording

The pulses from the five counters were delayed properly, mixed, then fed into a EG&G oscilloscope and recorded on film. Figure 9 shows typical pictures for the four types of events.

The film was projected by a Recordak PM-2 Projector on a screen with a magnification of 40. A thin line superimposed horizontally across the screen could be moved up and down. The position of the line was digitized and the number could be punched directly onto a paper tape by a machine made by Datex Co. in California. The information recorded on the tape was the height of the peaks of the five pulses and the base line of the pulse train. The data so recorded were then fed into a Burrough 220 high-speed digital computer at Caltech. The computer was programmed to obtain the pulse heights by subtracting the base line from the peak amplitudes of the pulses, to sort the pulses from each counter into a 50-channel pulse height spectrum, and to test the pulses of the pion counters against amplitude requirements for neutral and charged pions and the pulses of the nucleon counters against requirements for protons and neutrons. The output of the computer printed out the number of each of the four events, the number of rejected events, a 50-channel pulse height spectrum of each of the five counters for each of the four reactions and a 50-channel pulse height spectrum of each of the five counters including all events. Thus errors of manual measurement and record transfer were kept to a minimum. Figures 10 through 14 show the pulse height spectrum for each counter. The details of identification of reactions are presented in Section V.

The electronic circuits were calibrated two or three times

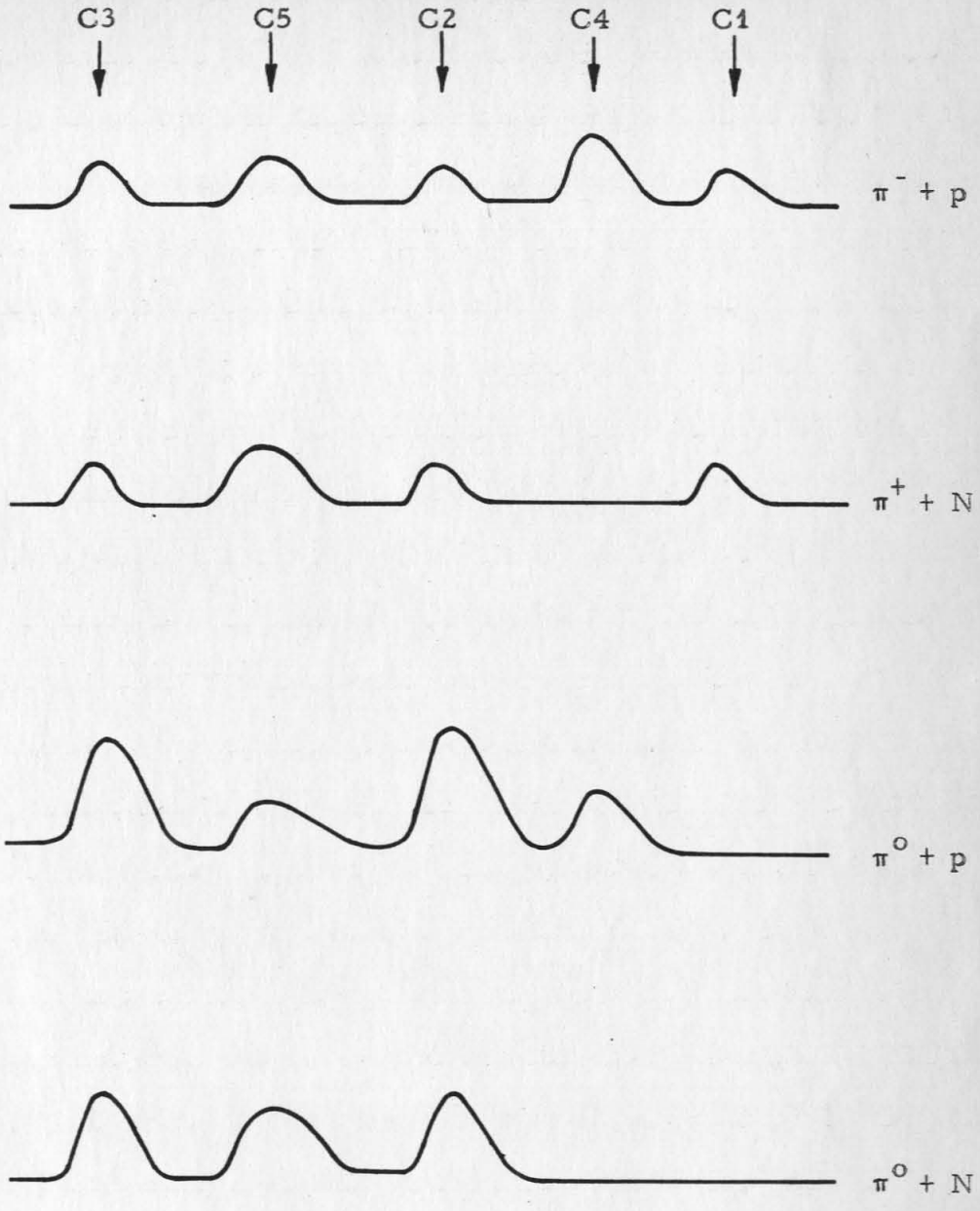

Typical Pulse Trains for the 4 Reactions

Figure 9

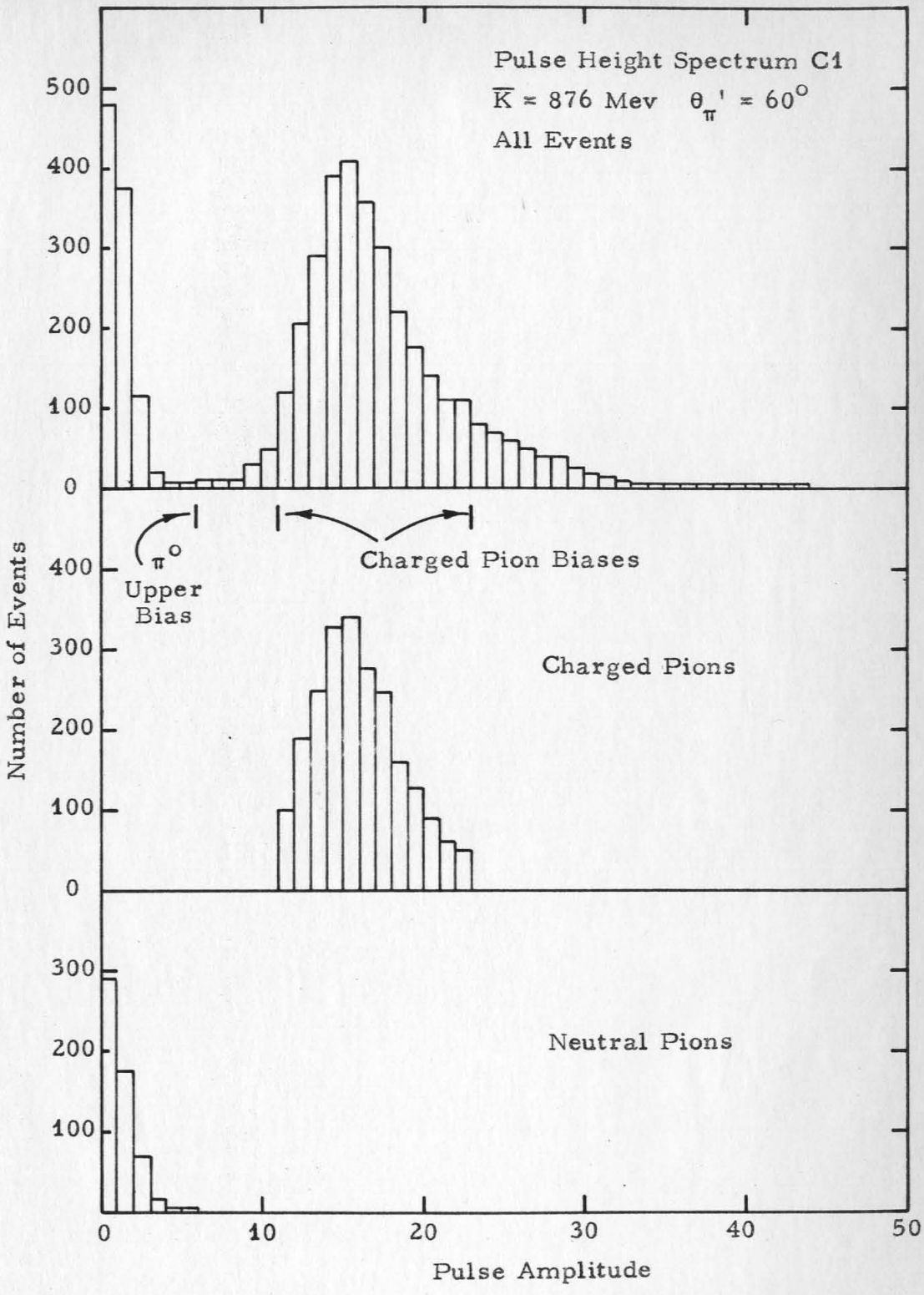
Pulse Height Spectrum C1
$\overline{K}$ = 876 Mev θ_π' = 60°
All Events
Charged Pion Biases
π^o
Upper
Bias
Charged Pions
Neutral Pions
Number of Events
Pulse Amplitude
0
100
200
300
400
500
10
20
30
40
50

Figure 10

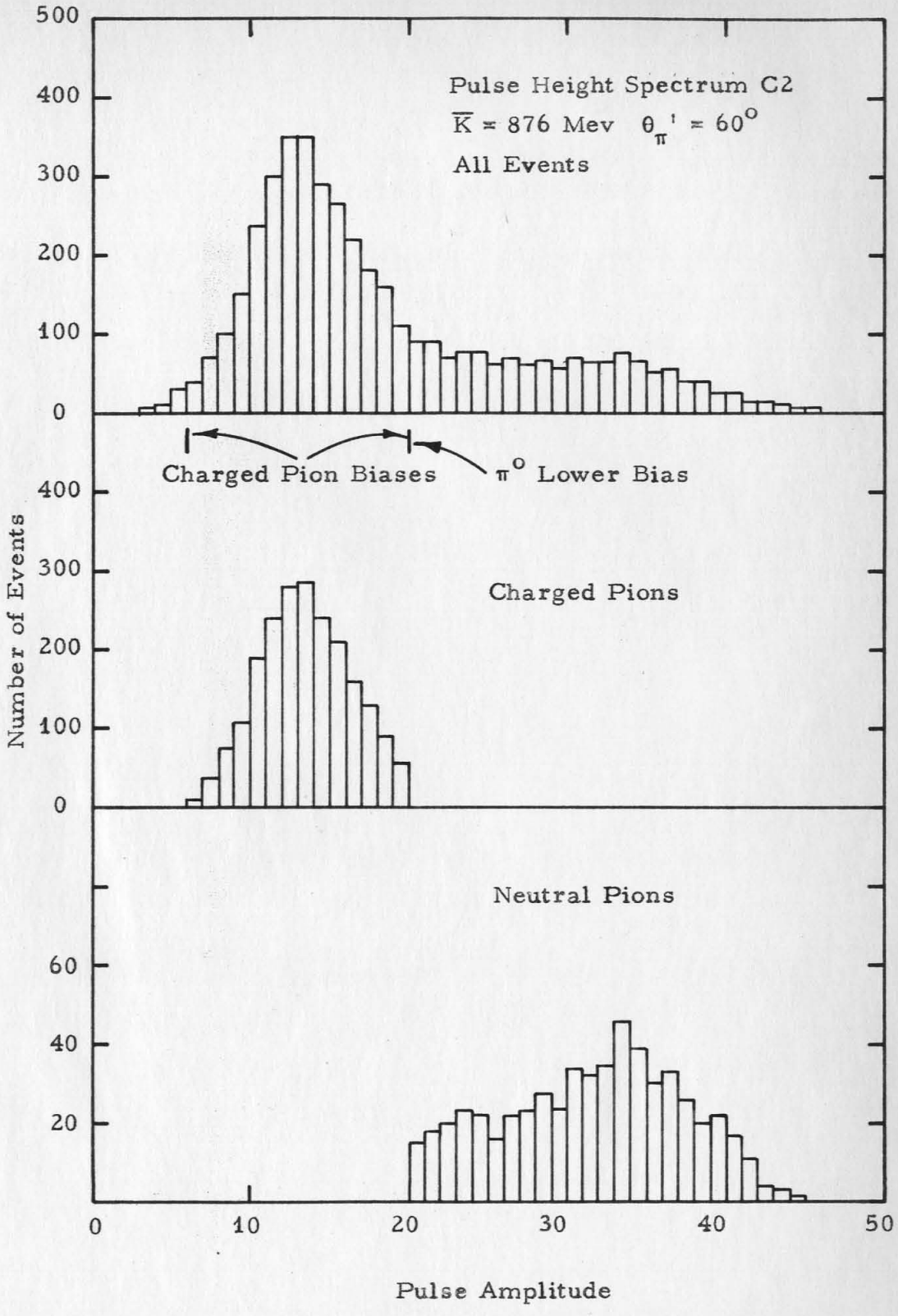
Pulse Height Spectrum C2
$\overline{K}$ = 876 Mev $\theta_\pi{}' = 60^o$
All Events
Charged Pion Biases
π^o Lower Bias
Charged Pions
Neutral Pions
Number of Events
Pulse Amplitude
500
400
300
200
100
0
60
40
20
10
30
50

Figure 11

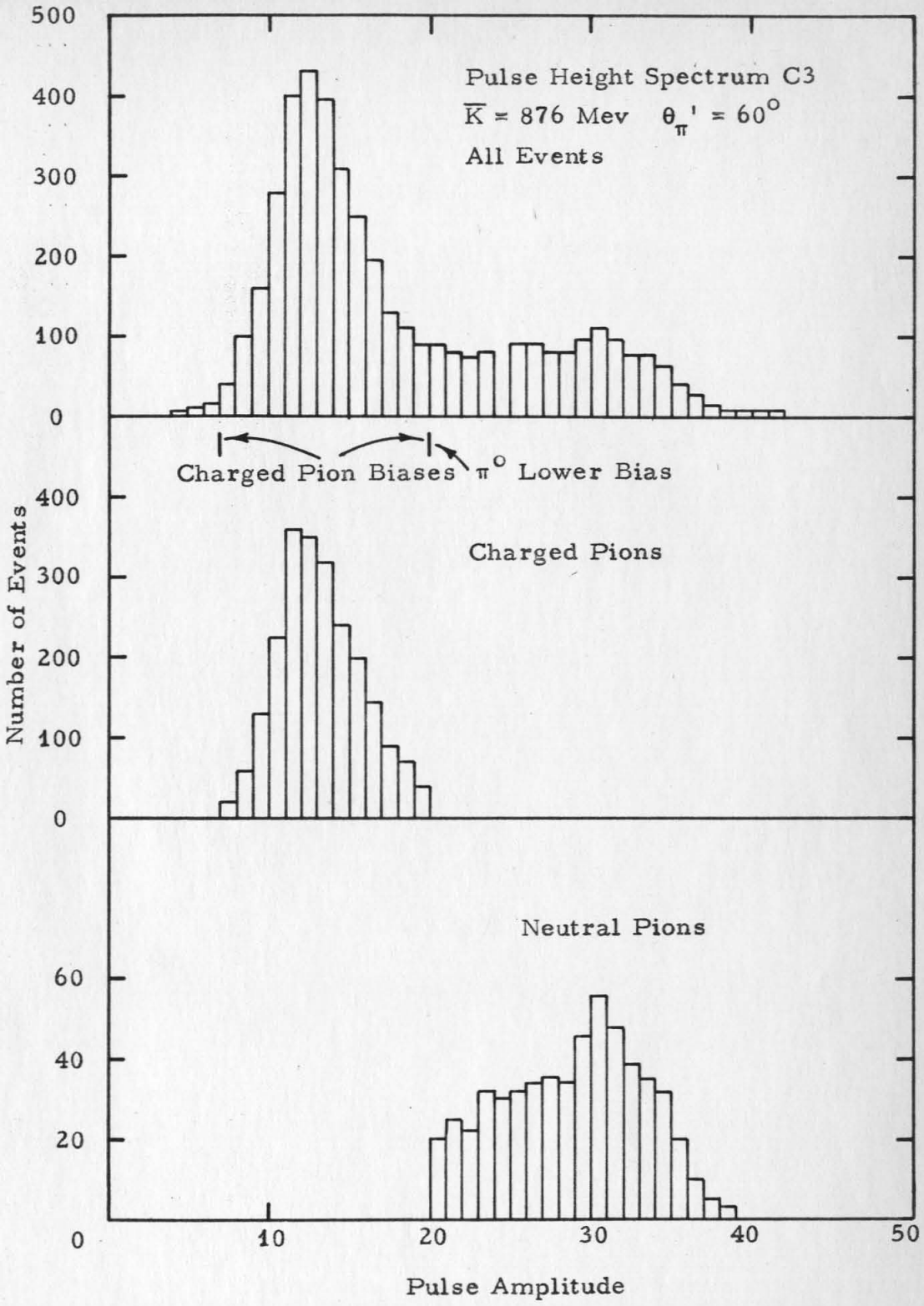
Pulse Height Spectrum C3
$\overline{K}$ = 876 Mev θ_π' = 60°
All Events
Charged Pion Biases
π^o Lower Bias
Charged Pions
Neutral Pions
Number of Events
Pulse Amplitude
500
400
300
200
100
0
60
40
20
10
30
50

Figure 12

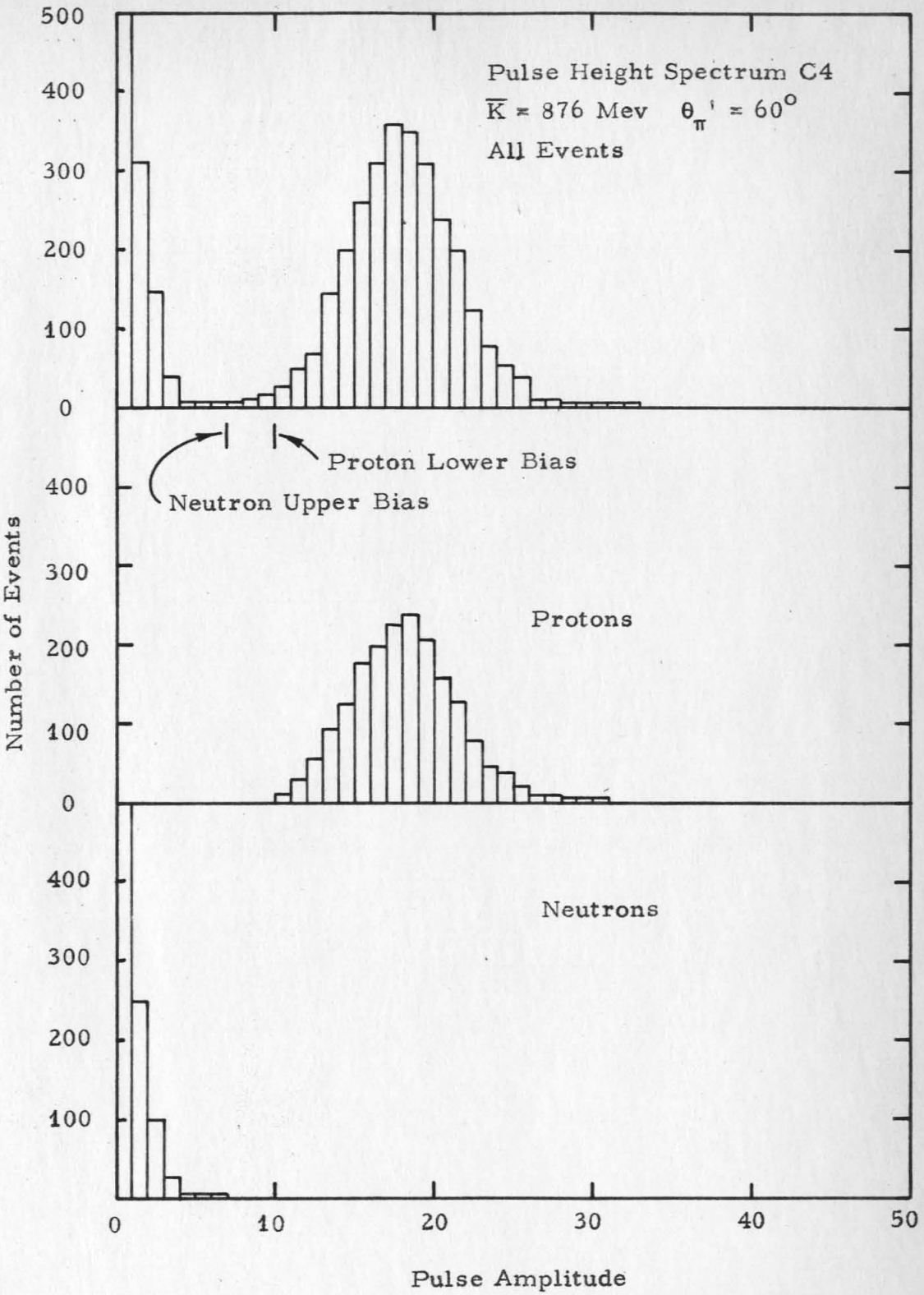
Pulse Height Spectrum C4
$\overline{K}$ = 876 Mev θ_π' = 60°
All Events
Proton Lower Bias
Neutron Upper Bias
Protons
Neutrons
Number of Events
Pulse Amplitude
500
400
300
200
100
0
0
10
20
30
40
50

Figure 13

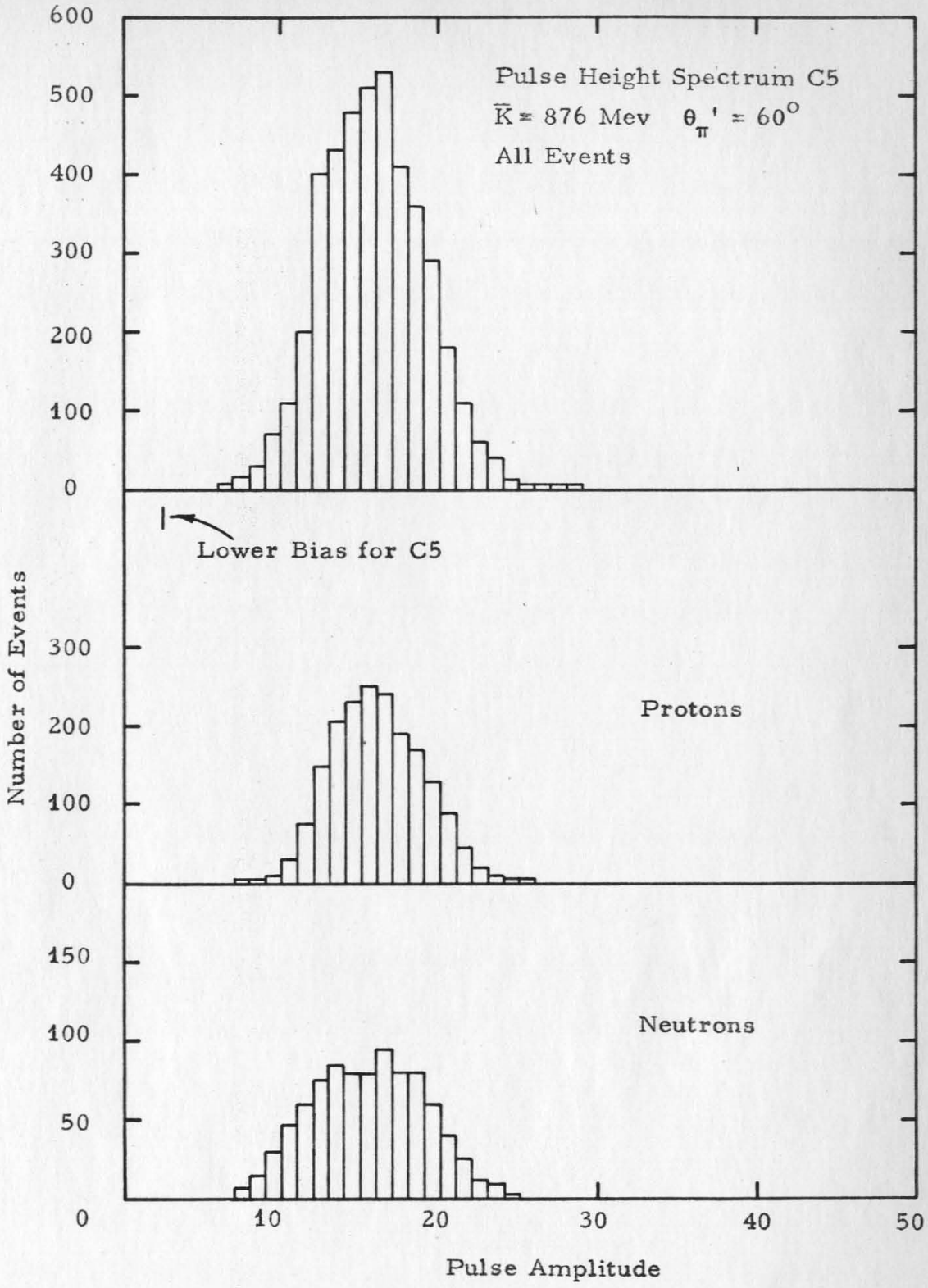
Pulse Height Spectrum C5
$\bar{K}$ = 876 Mev θ_π' = 60°
All Events
Lower Bias for C5
Protons
Neutrons
Number of Events
Pulse Amplitude
600
500
400
300
200
100
0
300
200
100
0
150
100
50
0
10
20
30
40
50

Figure 14

daily during data taking by feeding into the inputs of the two primary coincidence circuits standard pulses from a SKL mercury pulser. The upper and lower energy data were taken alternatively as often as possible in compromise with efficiency of the operation of synchrotron and convenience of other concurrent experiments. Ordinarily, the two sets of data were taken on alternate days. The stability of the high voltage on the phototubes and gain of the phototubes could be checked by their pulse height spectra and they showed very little shift. The target density was measured two or three times daily and an average used for the density. Individual measurements showed a difference of less than 1%. Pictures were developed normally within one day after they were exposed and on runs of slow counting rates three days after they were exposed.

V. DATA REDUCTION

A) Biases

As has been stated before, the signals from the five counters, properly delayed and mixed, were fed into an EG&G scope and recorded on film. The pulse height spectrum for each counter is shown in Figures 10 through 14. The peaks in the spectra for counters 1, 2, and 3 are those of charged pions; they have full width of 30% at half maximum. The peak in counter 4 is that of protons; it also has a full width of 30%. The peak in counter 5 is due to both protons and neutrons. It has a full width of 40% at half maximum due to

a) its large size, which means light may be reflected many times before striking phototubes;

b) the addition of three separate phototubes, even though extreme care was taken in balancing these phototubes, i.e. in obtaining equivalent output amplitudes when a particle struck the upper half of the counter as when it struck the lower half of the counter;

c) the broad energy spectrum of the charged particles produced from the neutron incident on the counter.

To identify the four reactions in this experiment, the following procedures were used.

1) Counter 5 was required to trigger the coincidence circuits. It had approximately 20% efficiency in converting neutrons (10). A bias set as shown in Figure 14 included all possible amplitudes. Pulses below this bias could not be resolved by the digitized scanner.

2) Counter 4 was used to distinguish protons from neutrons. Its 1/4" thickness had approximately 0.5% efficiency of converting a neutron. (10) The probability of converted charged products getting

into counter 5 could be estimated to be less than 20% from the geometry. The total efficiency for a neutron to look like a proton in both counters 4 and 5 was less than 0.1%. Biases A and B were set on counter 4 as shown in Figure 13. Pulses above bias B were identified as protons. Those below bias A were identified as neutrons.

3) In order to identify charged pions and neutral pions, biases were set on counters 1, 2, and 3. The pion for a particular event was identified as a charged pion or a neutral pion only if signals from all three counters satisfied the requirements set on each counter. As stated before, this was possible because the counting efficiencies cancelled out in the final result.

4) Counter 1 was used as a veto counter for neutral pions. We required no signal in this counter for a neutral pion. The probability that a photon from the decayed neutral pion be converted in the target or in the parafin shielding in front of the counters was 30%. An event such that counter 2 and counter 3 satisfied requirements for a neutral pion and counter 1 produced a signal was thrown out. This inefficiency could also be estimated experimentally. One could measure the ratio of events where all three counters satisfied the requirements for neutral pions to the events where only counters 2 and 3 were required to satisfy the biases for neutral pions. This turned out to be 61%. Charged pions, being minimum ionizing particles, show a peak in the spectrum. Biases for charged pions were set to include 90% of the area under the peak. The large pulses were excluded since these come mostly from neutral pions.

5) In counters 2 and 3, charged pions, being nearly minimum

ionizing particles, show a peak at the lower end of the spectrum. Photons from neutral pions, being converted by $1/2^{\pi}$ and $3/4^{\pi}$ of lead before reaching counters 3 and 2 respectively, have a spectrum which extends from the lower end of the spectrum for minimum ionizing particles to three times the pulse height of minimum ionizing particles. Thus spectra for charged and neutral pions overlap. A lower bias was set for charged pions to include all the charged pions and an upper bias was set for charged pions near the place where the two spectra intercept. A lower bias for neutral pions was set just above the upper bias for charged pions, and no upper bias was set for neutral pions. The effectiveness of these biases is indicated by the ratio of the number of the events where all three counters satisfy the requirements for neutral pions or charged pions to the number of the events where only counter C1 and one of the two counters C2 or C3 satisfy the requirements. The following table shows these ratios from data taken at $\theta^{1}_{\pi} = 60^{\circ}$ and photon energy between 800 and 950 mev.

$\pi^{\pm}$			π^{o}		
$\frac{N_{123}}{N_{12}}$	$\frac{N_{123}}{N_{13}}$	$\frac{N_{123}}{N_{23}}$	$\frac{N_{123}}{N_{12}}$	$\frac{N_{123}}{N_{13}}$	$\frac{N_{123}}{N_{23}}$
.95	.93	.83	.88	.81	.61

N_{123} is the number of events when biases are set on all three counters for the analysis. N_{12} is the number of events when biases are set only on counter C1 and C2. N_{13} and N_{23} have similar definitions as N_{12}.

An estimate of absolute counting efficiencies for neutral pions and neutrons is shown in Appendix I.

Before the above mentioned procedures were used to analyze the data, they were checked by data taken with hydrogen as target. Since hydrogen contains only free protons, only the following two reactions are possible,

1) $\gamma + p \rightarrow p + \pi^o$

2) $\gamma + p \rightarrow n + \pi^+$

plus a small amount of the pair productions

3) $\gamma + p \rightarrow p + \pi^+ + \pi^-$

4) $\gamma + p \rightarrow p + \pi^o + \pi^o$

5) $\gamma + p \rightarrow n + \pi^o + \pi^+$

The results of the hydrogen runs are shown in Table 4. A considerable amount of pair production of charged pions was detected. The ratio of the number of pair production of charged pions detected to the number of single production of positive pions range from 0.10 to 0.20.

A correction was made on this ratio for the possibility that a neutral pion might look like a charged pion. Details of the calculation are shown in Appendix V.

These corrected values of the ratio of the hydrogen runs are compared with the expected values for the ratio obtained from a calculation using the data of pair production of charged pions of Chasan et al. (12). The details of this calculation are shown in Appendix II, and the results are shown in Table 10 in Appendix II. The fact that a fairly good agreement was obtained indicates that

Table 4

Hydrogen Runs

Point	E_{01} (mev)	θ'_π	T (n sec)	BIPS	Counts						
					$\pi^o p$	$\pi^\pm p$	$\pi^o N$	$\pi^+ N$	$"\pi^\pm p"$*	$\frac{\pi^\pm p - "\pi^\pm p"}{\pi^+ N}$	$\frac{\pi^o N}{\pi^+ N}$
1	1150	60^o	27.4	990	156	37	2	205	3	$.16 \pm .03$	.010
2	950	60^o	31.4	802	193	38	0	245	6	$.13 \pm .02$	0
3	800	60^o	35.4	282	61	10	1	98	2	$.08 \pm .02$	.010
4	1150	90^o	32.5	775	131	33	1	148	5	$.19 \pm .04$	.007
5	950	90^o	32.5	1632	135	22	1	128	5	$.13 \pm .03$	.008

* $"\pi^\pm p"$ is the number of events of $\pi^o p$ that look like $\pi^\pm p$ by calculation.

the biases were properly chosen.

B) Corrections

a) Pion Pair Contaminations

There are three types of pion pair contamination. First, the nucleon counters may detect one of the pions and the pion counters detect the other. Second, the nucleon counters may detect one of the pions and the pion counters detect the nucleon. Third, the nucleon counters may detect the nucleon and the pion counters detect one of the pions. The first two types of contaminations did not exist. For most of the experimental points, kinematics ruled out such contaminations; for the rest of the points, the coincidence circuits eliminated such contaminations even though they were kinematically possible. For the third type of pair contamination, there are the following reactions.

(1) $\gamma + p \rightarrow p + \pi^+ + \pi^-$ (σ^{+-})

(2) $\gamma + p \rightarrow p + \pi^o + \pi^o$ (σ^{oo})

(3) $\gamma + p \rightarrow n + \pi^+ + \pi^o$ (σ^{+o})

(4) $\gamma + n \rightarrow n + \pi^+ + \pi^-$ (σ^{n+-})

(5) $\gamma + n \rightarrow n + \pi^o + \pi^o$ (σ^{noo})

(6) $\gamma + n \rightarrow p + \pi^- + \pi^o$ (σ^{n-o})

Thus reactions (1) and (6) may give contaminations to the single pion production $\gamma + n \rightarrow p + \pi^-$

reaction (2) to the reaction $\gamma + p \rightarrow p + \pi^o$

reactions (4) and (3) to the reaction $\gamma + p \rightarrow n + \pi^+$

and reaction (5) to the reaction $\gamma + n \rightarrow n + \pi^o$.

Corrections for pair productions in deuterium have been calculated in a similar manner as for pair productions in hydrogen. The quantities that were calculated were f^+, f^-, f^{no}, and f^o where f^+ is the ratio of the number of events of pair production in which a charged pion and a neutron were detected to the number of events of single production of positive pions. f^-, f^{no}, and f^o have similar definitions as f^+. Thus the observed counting rate of each reaction is to be corrected by a factor of 1 - f for that reaction.

In order to simplify the calculation, the effects of the internal motion of the nucleons in deuterium were ignored. The errors in f introduced by this simplification are expected to be less than 50%. Since the values of f are expected to be small as compared with the statistical errors of this experiment, this simplification is justifiable.

Since no data exists on the branching ratios of the pair production of pions, the assumption was made that the total isotopic spin state $I = 1/2$ dominates in the energy range of this experiment, and the interaction of the nucleon and one of the pions is dominated by $I = 3/2$ state. Thus the ratio of $\sigma^{+-} : \sigma^{oo} : \sigma^{+o}$ is 10 : 4 : 4 (16). This assumption is probably not correct; however, it seems to be more reasonable than the assumption that all pair productions have roughly the same cross sections since the preliminary work on pion pair productions at Cornell indicates that the reaction $\gamma + p \rightarrow p + \pi^+ + \pi^-$ occurs much more often than the reaction $\gamma + p \rightarrow p + \pi^o + \pi^o$ (17), and the latter reaction occurs about as often as the reaction $\gamma + p \rightarrow n + \pi^+ + \pi^o$ (18).

We also assumed in the calculation that protons and neutrons are equivalent in the pair production; that is to say $\sigma^{+-} = \sigma^{n+-}$, $\sigma^{oo} = \sigma^{noo}$, and $\sigma^{+o} = \sigma^{n-o}$.

The results of this calculation are shown in Table 5, where $f_T = \frac{(1-f^{no})(1-f^{-})}{(1-f^{o})(1-f^{+})}$ is the total correction factor. The values of the total correction factor range from .95 to .99. They are small compared to the statistical errors of this experiment. Details of this calculation are shown in Appendix III.

b) Target Contamination

A correction was necessitated by the hydrogen contamination in the deuterium. The result of an analysis made with a mass spectroscope by Smith-Emery Laboratory in Los Angeles is shown in the following table.

Hydrogen	0.51%
Hydrogen Deuteride	1.41%
Deuterium	98.08%
	100.00%

Since $\gamma + n \rightarrow n + \pi^o$ cannot be produced in hydrogen, the observed ratio of counting rates from deuteron can be written

$$\frac{C^{no}}{C^{o}} = \frac{C^{no}(D_2)}{C^{o}(D_2) + C^{o}(H_2)}$$

$$= \frac{C^{no}(D_2)}{C^{o}(D_2)} \frac{1}{1 + \frac{C^{o}(H_2)}{C^{o}(D_2)}}$$

Here $C^{o}(D_2)$ is the counting rate of the reaction $\gamma + p \rightarrow p + \pi^o$ for

Table 5

Pair Corrections

Point	f^+	f^-	f^{no}	f^o	f_T
1	.02	.05	.05	.03	.95
2	.03	.06	.05	.04	.96
2^1	.03	.06	.06	.05	.96
3a	.02	.02	.03	.02	.99
3b*	.02	.02	.03	.02	.99
3^1	.02	.03	.04	.03	.98
4*	.04	.09	.05	.06	.96
5*	.03	.07	.02	.01	.95

* no $\frac{1}{2}$" lead plate in front of C5

For definition of point 2^1 and 3^1 see Section VI

deuterium in the target and $C^o(H_2)$ is the counting of the reaction $\gamma + p \rightarrow p + \pi^o$ for the hydrogen contamination in the target.

$$\frac{C^{no}(D_2)}{C^o(D_2)} = \frac{C^{no}}{C^o}\left(1 + \frac{C^o(H_2)}{C^o(D_2)}\right)$$

$$= \frac{C^{no}}{C^o} D^o$$

$$D^o = 1 + \frac{\text{number of free protons}}{\text{number of bound protons}} \cdot g^o$$

where $g^o = C^o{}_H / C^o{}_D$ is the ratio of counting rates for the hydrogen run to that for the deuterium run at each experimental point. It measures the loss of counting rate for deuteron due to the internal motion of the nucleons in the deuteron.

Similarly for the ratio C^-/C^+

$$\frac{C^-(D_2)}{C^+(D_2)} = \frac{C^-}{C^+} D^+$$

$$D^+ = 1 + \frac{\text{number of free protons}}{\text{number of bound protons}} \cdot g^+$$

where $g^+ = C^+{}_H / C^+{}_D$

Thus

$$\frac{\sigma^{no}}{\sigma^o} = \frac{C^{no} C^- \sigma^+}{C^o C^+ \sigma^-} D^o D^+$$

The values of D^o, D^+, and $D^o D^+$ for each experimental point are shown in the following table.

Point	D^o	D^+	$D^o D^+$
1	1.020	1.020	1.04
2	1.034	1.024	1.06
3	1.039	1.029	1.07
4	1.018	1.020	1.04
5	1.029	1.021	1.05

c) Accidentals

Accidental coincidences in this experiment were measured by adding 100 nanoseconds delay to counter 5. Since the beam of the synchrotron has a period of 25 nanoseconds between its maximum intensity due to the fact that the R.F. system has a frequency of 40 megacycles, it was necessary to use a delay of multiples of 25 nanoseconds in order to measure the accidentals. The result is shown in Table 6 where the name "electronic accidental" is given to the accidental triggering of the coincidence circuit system by a single large pulse. The "electronic accidental" is characterized on the film by the absence of the signal from either C2, C3 or C5. Since no pictures were taken for the accidental runs, the values for the "electronic accidentals" were obtained from the regular runs immediately preceding and following the accidental runs by counting the number of events in which the signal from either C2, C3 or C5 was missing. It is obvious no correction for accidentals is necessary.

d) Background

Empty target background in this experiment was expected to be very small since the 0.030" thick steel hemispheres at two ends of the target were shielded from the counters. Table 7 shows the percentage of background as compared to foreground counting rate. They are too small to be counted in view of the large statistical errors of this experiment.

C) Deuterium Dynamics Calculation

The synchrotron subtraction procedure defines an average photon energy in the laboratory system for each experimental point.

Table 6

Accidentals

E_o (mev)	θ'_π	BIPS	Counts	A^*	B^+	$\frac{A-B}{BIP}^{++}$	Total number of reactions	$\%\frac{A-B}{Total}$
800	60^o	310	5	.002	.004	$-.002^{+++}$	.466	$-4\%^{+++}$
700	60^o	370	2	.0005	0	-.0005	.233	2%
950	90^o	120	0	0	0	0	.468	0%

* A = $\frac{\text{Total Accidental}}{\text{BIP}}$

$^+$ B = $\frac{\text{"Electronic Accidental"}}{\text{BIP}}$

$^{++}$A-B = $\frac{\text{True Accidental}}{\text{BIP}}$

$^{+++}$ due to statistics

Table 7

Background

E_o (mev)	θ'_π	BIPS	Counts	Background/BIP	Total counts/BIP	% $\frac{\text{Background}}{\text{Total}}$
800	60^o	150	2	.001	.466	2%
950	60^o	150	1	.001	.481	2%
1150	60^o	100	1	.001	.910	1%
950	90^o	120	0	0	.468	0%

However, it is most interesting to express the result in terms of an average photon energy $\overline{K}$ in the rest system of the nucleon. Due to the internal motion of the nucleon in the deuteron, the energy of a photon which initiates a certain reaction is different for the two coordinate systems. Thus the average photon energy $\overline{K}$ for each point in the rest system of the nucleon is different from the average energy $\overline{k}$ in the laboratory system.

To calculate the average energy, it is necessary to calculate the deuterium resolution functions for upper and lower synchrotron end point energies for each experimental point, then subtract the resolution function of the lower end point energy from that of the upper end point energy and use the difference as a weighting function in calculating the average energy.

The calculation of the resolution function follows closely that of Neugebauer and Wales (9). The deuterium nucleus is assumed to satisfy the "spectator" model when it interacts with the photon, i.e. the photon interacts with just one of the nucleons in the deuteron while the other nucleon remains a "spectator" and is not involved in the interaction. Furthermore, this spectator nucleon is assumed to have the same momentum distribution in the final state as it had while a bound particle inside the deuteron.

The resolution function is defined as the relative probability for a photon with an energy K in the nucleon rest system to produce a recoil nucleon with laboratory momentum P_N and laboratory angle θ_N taking account of the finite resolution of the coincidence circuits, the angular resolution of the counters, and the form of the bremsstrahlung spectrum if the pion photoproduction cross section in the CM system is assumed to be independent of energy within

the energy range of interest.

The counting rate per BIP of nucleons with momentum P_N at laboratory angle θ_N capable of being accepted by the coincidence circuits is

$$C = \frac{NW}{E_o} \overline{\sigma(\theta')} \int_{\underline{P}_T} \int_K \frac{d\Omega'_N}{d\Omega_N} \frac{b(k/E_o)}{k} \Delta\Omega_N$$

$$\rho^\pi \rho^N \eta^{\pi N}(k) \epsilon(\theta_\pi) h(P_T) dP_T \frac{d\Omega_T}{4\pi} dK$$

where N, $\frac{d\Omega'_N}{d\Omega_N}$, $\Delta\Omega_N$, $\frac{W}{E_o} \frac{b(k/E_o)}{k}$, and $h(P_T)dP_T \frac{d\Omega_T}{4\pi}$ have been defined before. $\overline{\sigma(\theta')}$ is the average differential cross section in the CM system within the energy interval of the coincidence circuits. $\eta^{\pi N}(k)$ is the resolution of the coincidence circuits as shown in Figure 7. $\epsilon(\theta_\pi)$ is a function equal to one if the outgoing pion is emitted within the angular range of the pion counters, zero if not.

The above expression for C is still too complicated to be evaluated analytically, but a numerical calculation can be made following a method used by Smythe (13) who has calculated the momentum distribution of the nucleons in deuterium using both Gartenhaus and Hulthen wave functions which give essentially equal results as shown in Figure 15. Two hundred equally probable values of p_T are selected and C is represented as a sum over these two hundred points.

$$C = \overline{\sigma(\theta')} \frac{W}{E_o} \frac{N}{200} \sum_{\underline{P}_T} \int_K \frac{d\Omega'_N}{d\Omega_N} \frac{b(k/E_o)}{k} \Delta\Omega_N \eta^{\pi N}(k) \epsilon(\theta_\pi) dK$$

The sum over the two hundred configurations obviously includes contribution from a large range of photon energies. Thus a large region of K-space is divided into appropriate discreet intervals and the integrand

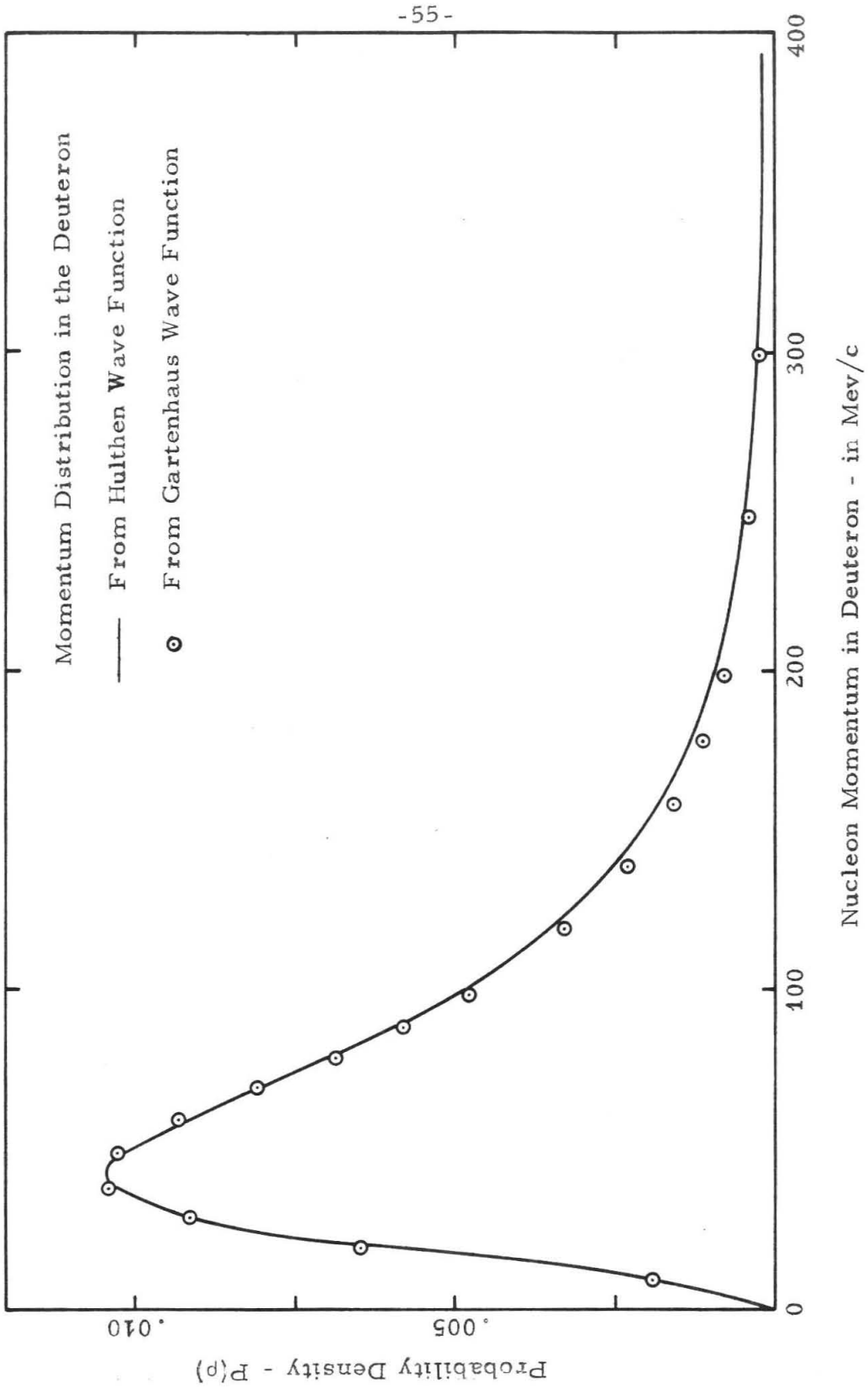
Momentum Distribution in the Deuteron
From Hulthen Wave Function
From Gartenhaus Wave Function
Probability Density - P(p)
.010
.005
0
100
200
300
400
Nucleon Momentum in Deuteron - in Mev/c

Figure 15

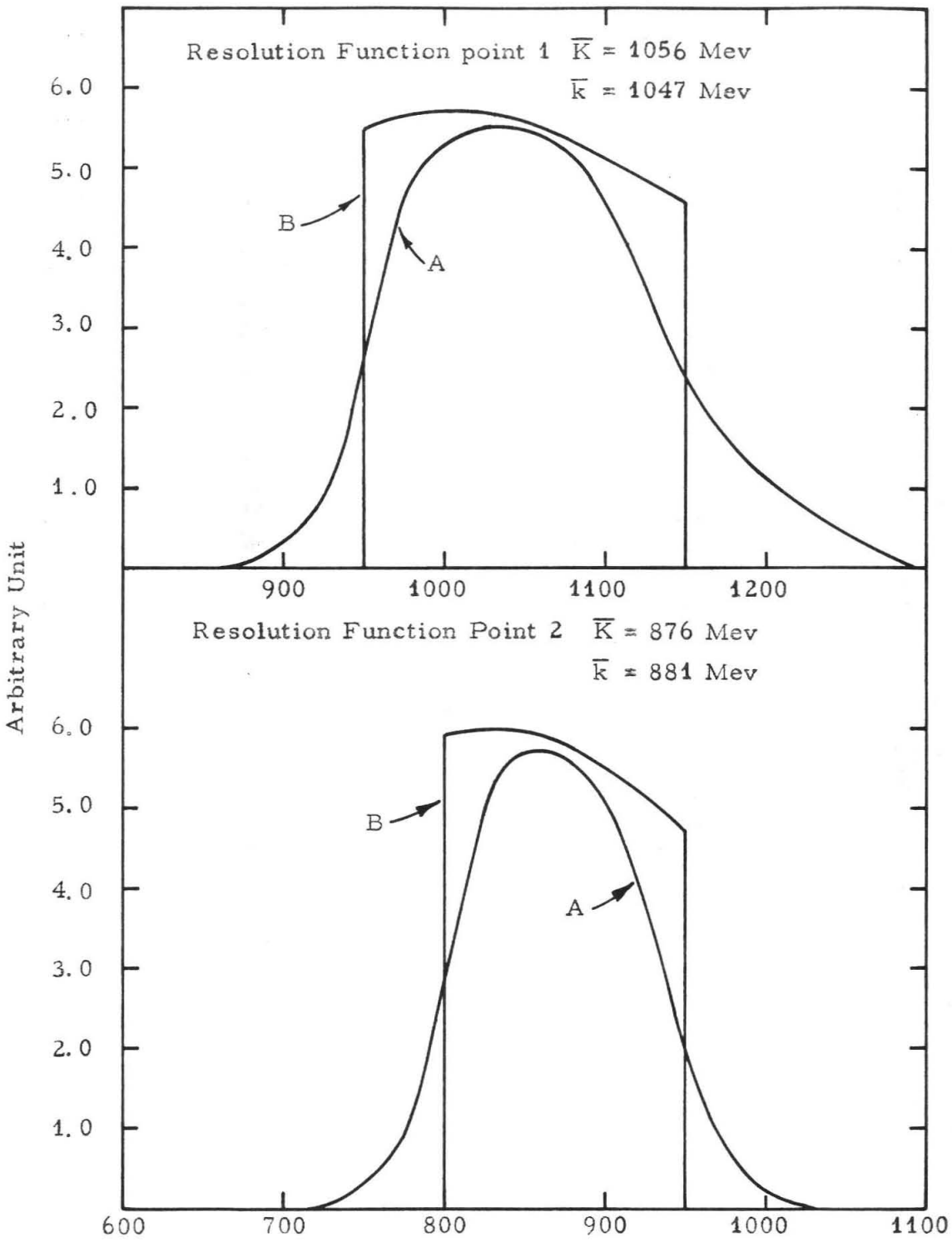
Resolution Function point 1 $\bar{K}$ = 1056 Mev
$\bar{k}$ = 1047 Mev
B
A
6.0
5.0
4.0
3.0
2.0
1.0
900
1000
1100
1200
Resolution Function Point 2 $\bar{K}$ = 876 Mev
$\bar{k}$ = 881 Mev
B
A
6.0
5.0
4.0
3.0
2.0
1.0
600
700
800
900
1000
1100
Arbitrary Unit
K or k (Mev)

Figure 16

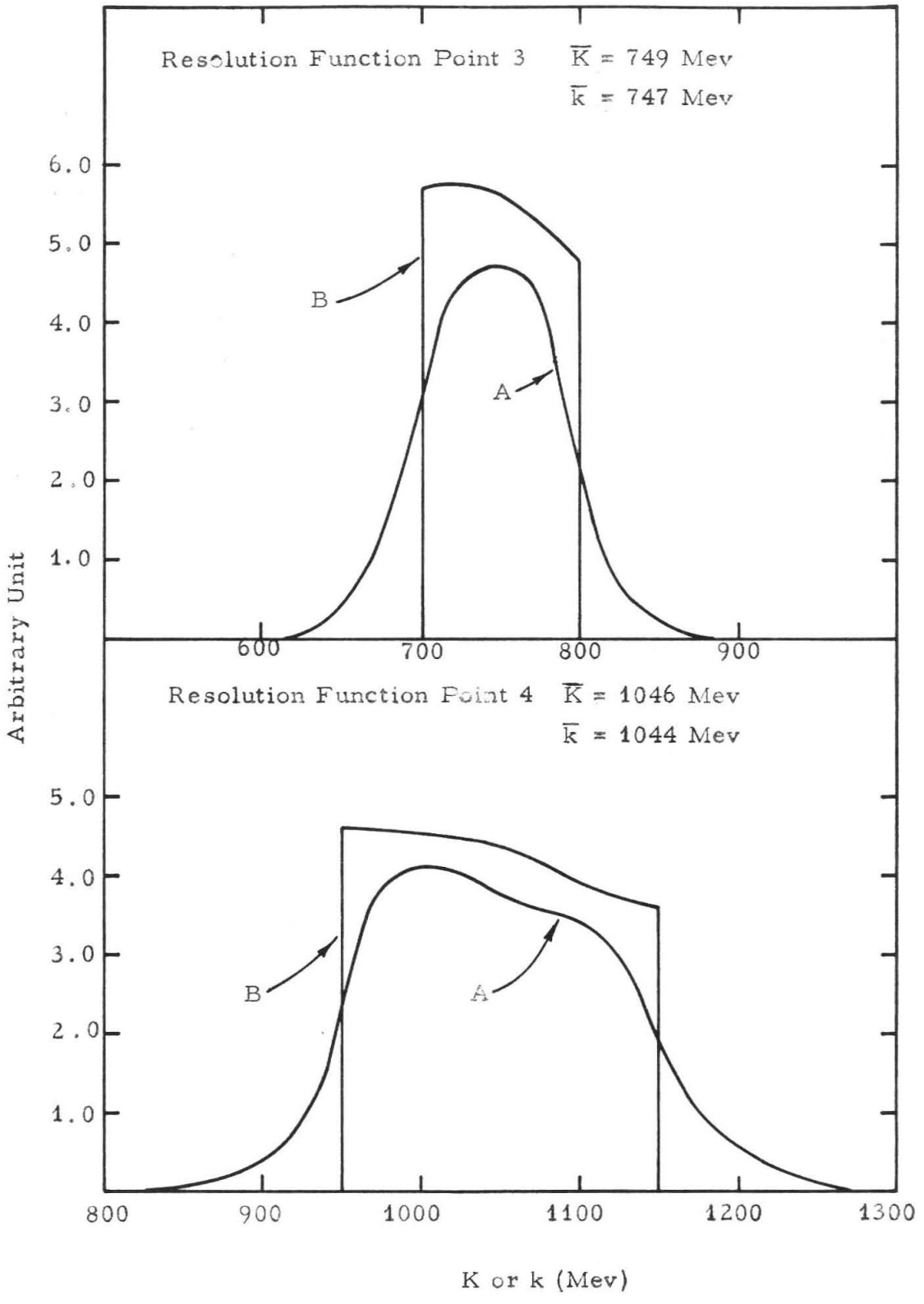
Resolution Function Point 3
$\overline{K}$ = 749 Mev
$\overline{k}$ = 747 Mev
6.0
5.0
4.0
3.0
2.0
1.0
B
A
600
700
800
900
Resolution Function Point 4
$\overline{K}$ = 1046 Mev
$\overline{k}$ = 1044 Mev
5.0
4.0
3.0
2.0
1.0
B
A
800
900
1000
1100
1200
1300
Arbitrary Unit
K or k (Mev)

Figure 17

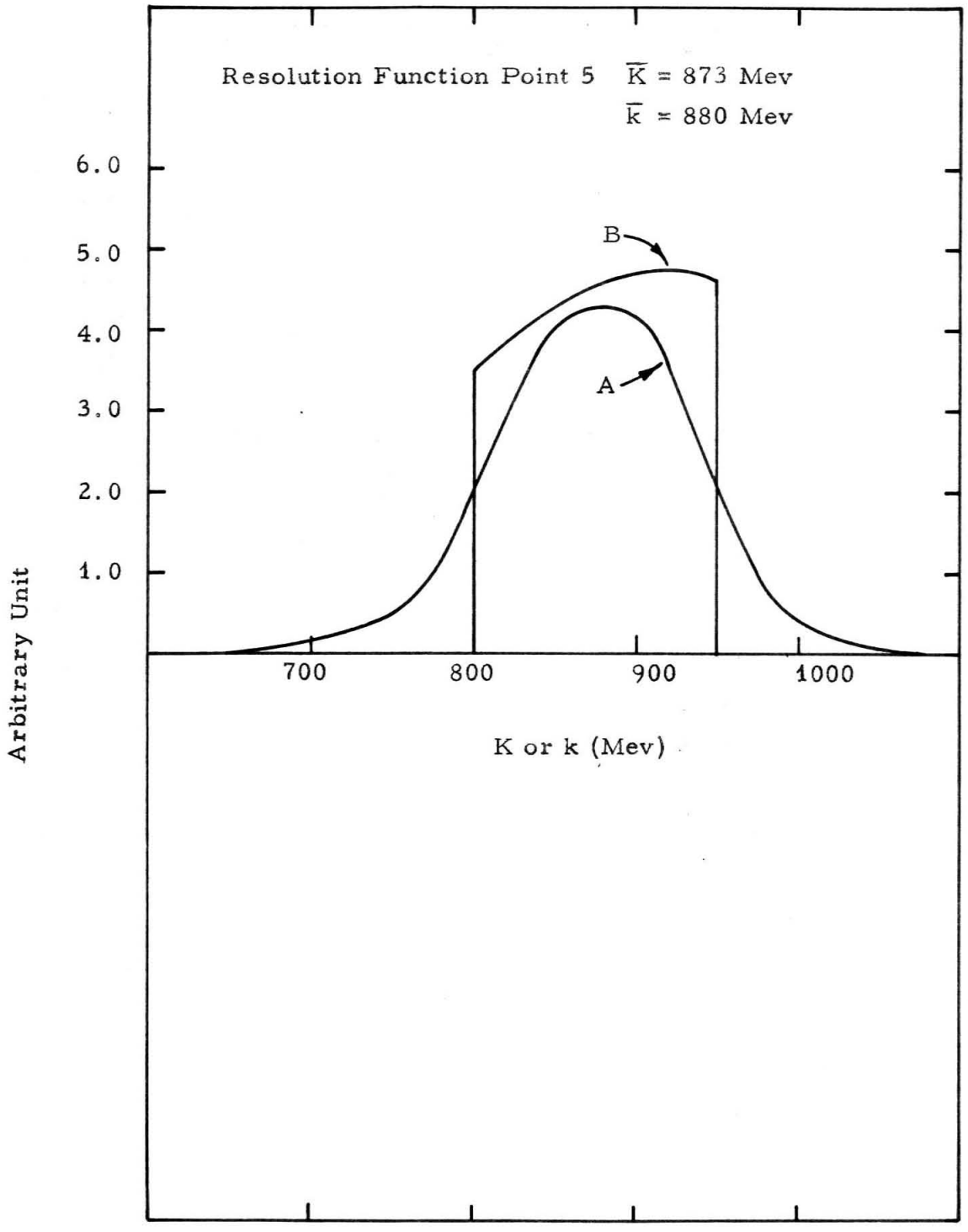
Resolution Function Point 5 $\bar{K}$ = 873 Mev
$\bar{k}$ = 880 Mev
6.0
5.0
4.0
3.0
2.0
1.0
B
A
700
800
900
1000
K or k (Mev)
Arbitrary Unit

Figure 18

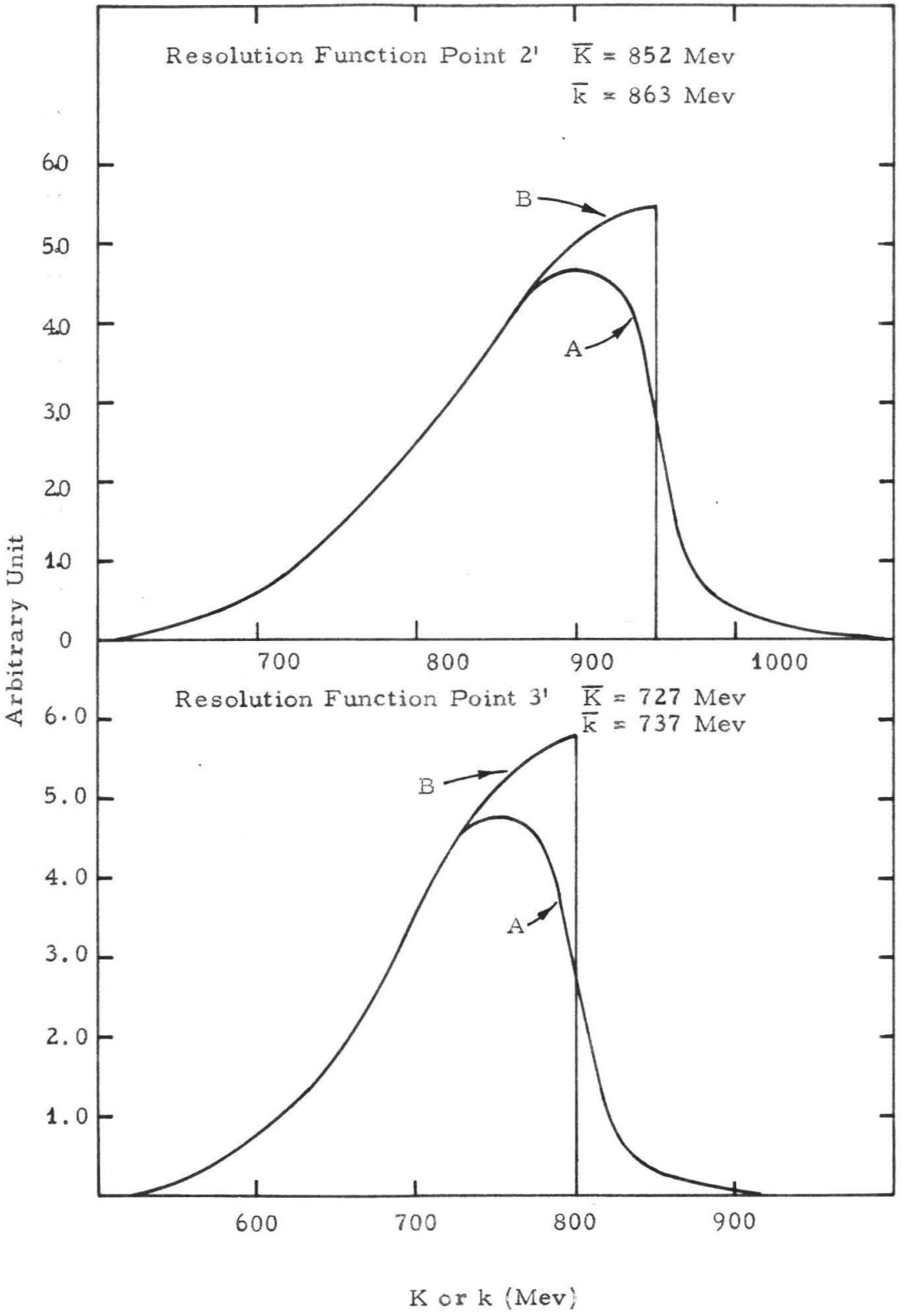
Resolution Function Point 2' $\overline{K}$ = 852 Mev
$\overline{k}$ = 863 Mev
B
A
6.0
5.0
4.0
3.0
2.0
1.0
0
700
800
900
1000
Resolution Function Point 3' $\overline{K}$ = 727 Mev
$\overline{k}$ = 737 Mev
B
A
6.0
5.0
4.0
3.0
2.0
1.0
600
700
800
900
Arbitrary Unit
K or k (Mev)

Figure 19

$$\frac{d\Omega'_N}{d\Omega_N} \frac{b(k/E_o)}{k} \Delta\Omega \eta^{\pi N}(k) \epsilon(\theta_\pi)$$

is evaluated at the interval midpoint for each of the two hundred configurations. The sum of the integrands at a given K gives the relative contribution to the counting rate of photons of energy K.

The resolutions as a function of photon energy K are shown as Curve A in Figures 16 through 19. Curve B in each figure is the resolution as a function of photon energy k in the laboratory system. The details of the calculation, except for $\eta^{\pi N}(k)$ and $\epsilon(\theta_\pi)$, are similar to that of Neugebauer (9). The appearance of point $2'$ and $3'$ will be explained in the next section.

The calculation of the average emission angle of the pion in the CM system of the target nucleon and the incident photon is extremely lengthy. In view of the large statistical errors of our data and the close proximity of $\overline{K}$ and $\overline{k}$, the calculation has not been done. All data are expressed in terms of θ'_π the average emission angle of the pions in the CM system when the nucleons in the deuterium are assumed to be at rest in the laboratory system.

VI. RESULTS

Counting rates for this experiment are shown in Table 8. E_o is the synchrotron end point energy. θ'_π is the average emission angle of the pions in the CM system as defined before. T is the delay of C5 with respect to C2 and C3. The counting rates are expressed in "normalized equivalent quanta". The word "normalized" refers to the fact that the counting rate is normalized to unit target density. The term "equivalent quanta" refers to the fact that the counting rate is normalized to an energy flux in the beam equal to the maximum photon energy.

The results of this experiment, taking account of all corrections, are shown in Table 9 and plotted in Figure 20. Each experimental point is identified by $\overline{K}$, the average energy of the photons in the rest system of the nucleon and θ'_π. σ^+/σ^-, the ratio of the cross section for photoproduction of positive pions from protons to that of negative pions from neutrons is obtained from the experiment of Neugebauer and Wales (3) by interpolation.

The differential cross sections for the photoproduction of neutral pions from neutrons are derived by multiplying the ratios by the cross sections for photoproduction of neutral pions from protons obtained from the experiment of Diebold et al. (14). The results of such a calculation are also shown in Table 9 and plotted in Figure 21.

Data for point 2' were obtained while the synchrotron was running at the lower end point energy for point 1. For point 1, the delay on C5 was set at 27.4 ns with respect to C2 and C3. The data we use for point 1 were obtained by subtracting the 950 mev data

Table 8

Counting Rates of this Experiment

E_o (mev)	θ'_π	T (nsec)	Counts/100 BIPS				Counts/10^9 NEQ			
			$\pi^o p$	$\pi^- p$	$\pi^o N$	$\pi^+ N$	$\pi^o p$	$\pi^- p$	$\pi^o N$	$\pi^+ N$
1150	60^o	27.4	9.93±.32	22.9±.48	1.67±.13	13.3±.36	3.26±.10	7.53±.16	0.55±.043	4.36±.12
950	60^o	27.4	4.03±.23	13.9±.42	.85±.10	7.08±.30	1.01±.057	3.50±.10	0.21±.026	1.78±.074
950	60^o	31.4	8.45±.27	25.1±.46	1.80±.12	14.7±.35	2.08±.065	6.20±.11	0.44±.030	3.63±.088
800	60^o	31.4	3.76±.21	15.5±.43	.96±.11	10.3±.35	0.72±.040	2.97±.082	0.18±.020	1.97±.068
800	60^o	35.4	4.53±.27	17.2±.53	1.55±.16	14.7±.49	0.86±.052	3.26±.098	0.30±.030	2.79±.092
700	60^o	35.4	1.09±.16	5.30±.34	.79±.13	8.43±.43	0.19±.027	0.92±.059	0.13±.023	1.46±.073
800*	60^o	35.4	7.73±.38	44.5±.92	1.42±.16	16.8±.56	1.29±.063	7.44±.15	0.24±.027	2.81±.095
700*	60^o	35.4	2.14±.23	22.9±.77	.55±.13	7.54±.44	0.36±.040	3.88±.13	0.09±.020	1.28±.075
1150*	90^o	32.5	10.6±.32	31.7±.57	1.29±.11	10.6±.33	2.52±.077	7.51±.13	0.31±.026	2.50±.077
950*	90^o	32.5	3.72±.21	19.7±.48	.66±.09	4.93±.24	0.79±.045	4.21±.10	0.14±.018	1.05±.051
800*	90^o	32.5	0.85±.13	13.9±.53	.29±.08	2.5±.23	0.16±.025	2.56±.10	.054±.014	0.47±.043

*No 1/2" lead plate in front of counter 5.

Table 9

Results of this Experiment

Point	$\overline{K}$ (Mev)	θ_{π}'	$\frac{C^{no}C^{-}}{C^{o}C^{+}}$	f_T	$D^{o}D^{+}$	$\frac{\sigma^{+}}{\sigma^{-}}$	$\frac{\sigma^{no}}{\sigma^{o}}$	σ^{no} (μb/Sr)
1	1056	60^{o}	0.24±.041	.95	1.04	2.2±.022	0.52±.10	0.68±.13
2	876	60^{o}	0.37±.063	.96	1.06	1.9±.019	0.71±.14	0.92±.18
2'	852	60^{o}	0.41±.061	.96	1.06	1.75±.018	0.73±.13	1.09±.19
3a	749	60^{o}	0.44±.11	.99	1.07	1.4±.014	0.65±.17	1.62±.43
3b*	749	60^{o}	0.38±.10	.99	1.07	1.4±.014	0.57±.15	1.42±.37
3'	727	60^{o}	0.38±.053	.99	1.07	1.35±.014	0.54±.09	1.52±.26
4*	1046	90^{o}	0.22±.046	.96	1.04	2.1±.021	0.46±.10	0.64±.14
5*	873	90^{o}	0.39±.12	.95	1.05	1.6±.016	0.62±.20	1.24±.40

*No lead plate in front of C5.

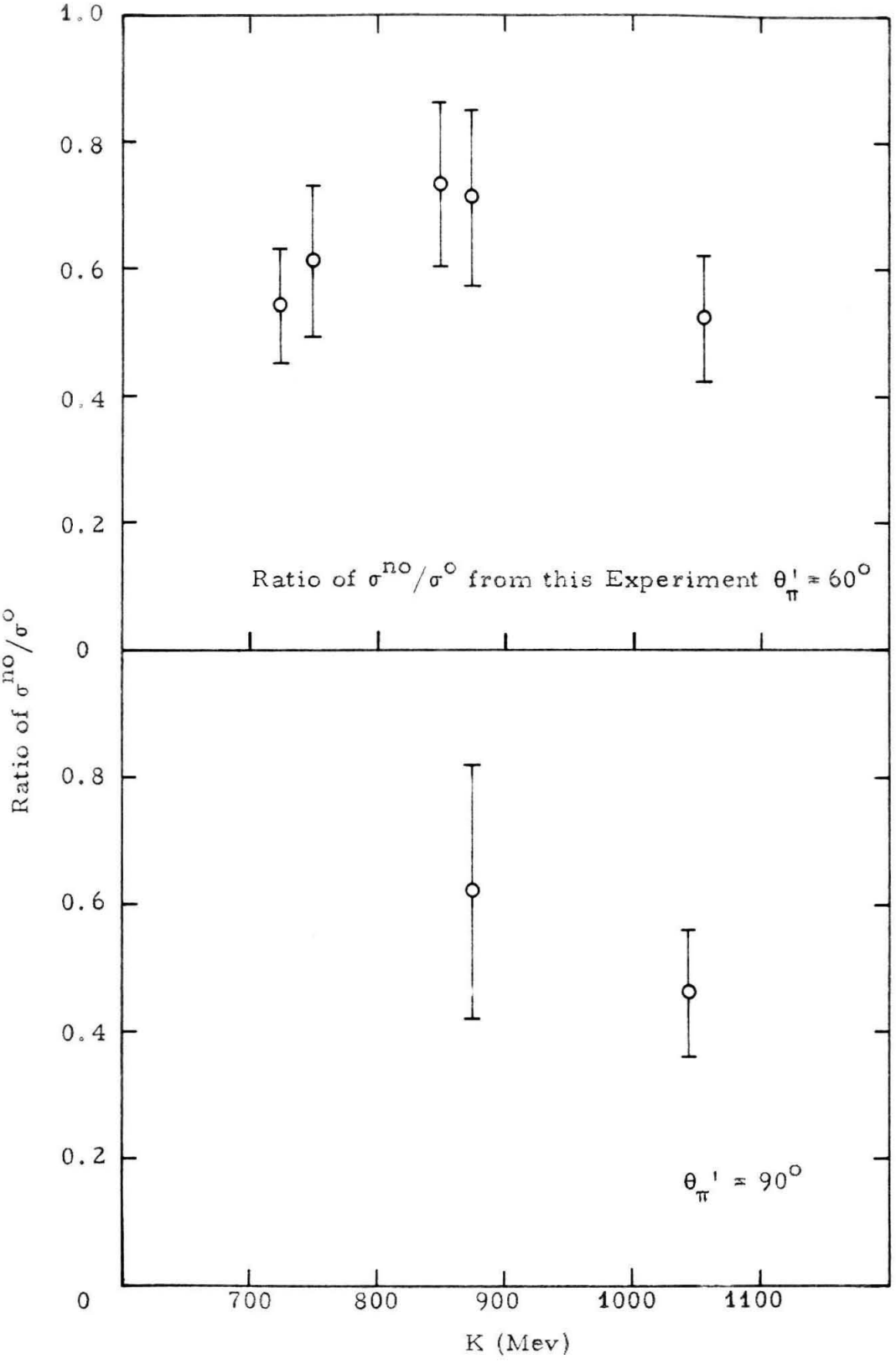
1.0
0.8
0.6
0.4
0.2
0
Ratio of σ^{no}/σ^{o} from this Experiment $\theta_\pi' \approx 60^o$
0.8
0.6
0.4
0.2
0
$\theta_\pi' \approx 90^o$
Ratio of σ^{no}/σ^{o}
700
800
900
1000
1100
K (Mev)

Figure 20

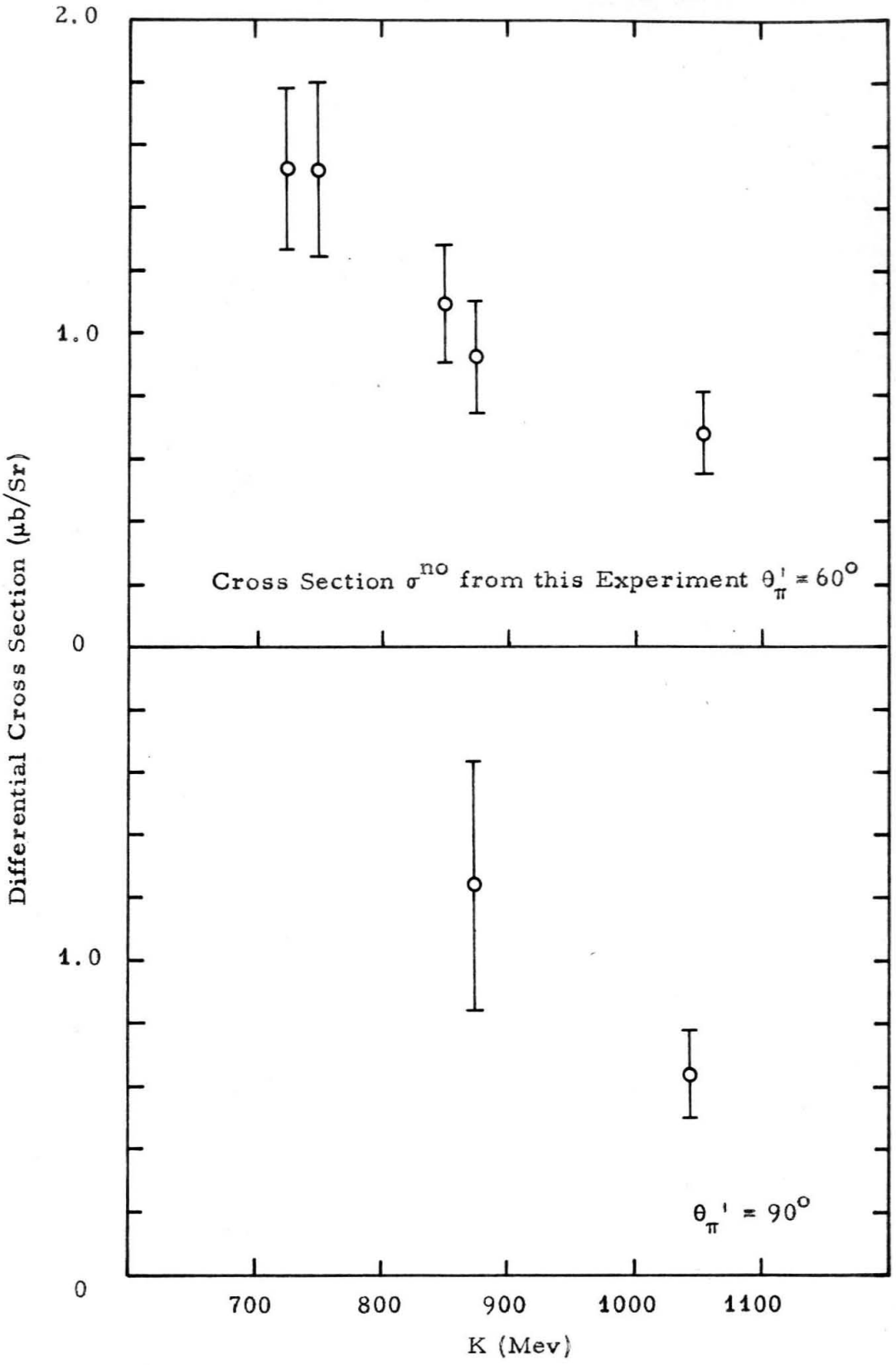
2.0
1.0
0
Cross Section σ^{no} from this Experiment $\theta_\pi' = 60^\circ$
1.0
0
$\theta_\pi' = 90^\circ$
700
800
900
1000
1100
K (Mev)
Differential Cross Section (μb/Sr)

Figure 21

fromthe 1150 mev data. As one can see from the resolution function plotted in Figure 19, the average photon energy of the data taken with the synchrotron running at 950 mev and delay set for point 1 is very close to the average photon energy of point 2 when the data were obtained by subtracting the 800 mev data from the 950 mev data with the delay of C5 set at 31.4 ns with respect to C2 and C3. Data for point $3'$ were obtained in a similar manner.

The fact that the results of points $2'$ and $3'$ agree with those of points 2 and 3, respectively, indicates that the ratio of σ^{no} to σ^{o} does not change rapidly within the energy interval of each point. Furthermore, it gives confidence in the working of the fast electronic circuits, and in the belief that efficiencies η's defined in Section II do not greatly affect the data. It indicates that even on the slope of the resolution of the coincidence circuits where the efficiency is not 100% the variation in the amplitudes of the input pulses does not materially affect the operation of the coincidence circuits.

One of the strengths of this experiment lies in the cancellation of many experimental errors when a ratio is measured. The errors which are quoted for the ratio are mostly statistical. In all cases, the corrections made are small compared to the statistical errors.

The results of this experiment can be summarized as follows:

1) The ratio of the differential cross section for photoproduction of neutral pions from neutrons to that of photoproduction of neutral pions from protons shows a maximum near 875 mev at $\theta'_{\pi} = 60^{o}$.

2) The ratio at each energy does not change very much between $\theta'_{\pi} = 60^{o}$ and $\theta'_{\pi} = 90^{o}$.

3) The differential cross section σ^{no} interpreted with the latest value of σ^{o} decreases from 1.52 at 750 mev to .68μb at 1150 mev at $\theta'_{\pi} \approx 60^{o}$ and from 1.24 at 875 mev to .64μb at 1150 mev at $\theta'_{\pi} \approx 90^{o}$.

4) No total cross section of $\gamma + n \rightarrow n + \pi^{o}$ as a function of energy was obtained.

VII. DISCUSSION

It has been shown by Watson (15) that the pion photoproduction amplitude can be expressed in terms of three matrix elements V_1, V_3 and S_1. The relations are

$$M^+ = \sqrt{2}\, V_3 + \sqrt{1/2}\, V_1 - \sqrt{2}\, S_1$$

$$M^o = 2\, V_3 - 1/2\, V_1 + S_1$$

$$M^- = \sqrt{2}\, V_3 + \sqrt{1/2}\, V_1 + \sqrt{2}\, S_1$$

$$M^{no} = 2\, V_3 - 1/2\, V_1 - S_1$$

The matrix elements V_3 and V_1 are isospin vectors and are for transitions leading to final states with $I = 3/2$ and $I = 1/2$ respectively. S_1 is an isospin scalar and leads to a final $I = 1/2$ state.

For a pure $I = 3/2$ state, such an analysis gives

$$\sigma^o : \sigma^{no} : \sigma^- : \sigma^+ = 2 : 2 : 1 : 1$$

For a pure $I = 1/2$ state

$$\frac{\sigma^{no}}{\sigma^o} = \frac{\sigma^-}{\sigma^+}$$

$$\sigma^+ : \sigma^o = 2 : 1$$

$$\sigma^- : \sigma^{no} = 2 : 1$$

Thus for a pure $I = 1/2$ state, isotopic spin considerations predict a unique relationship between σ^o and σ^+ but do not provide a unique relationship between σ^- and σ^+ or $\sigma^{no} : \sigma^o$ unless it can be shown that either S_1 or V_1 is zero.

Figure 22 shows the results of Neugebauer and Wales for the

σ^-/σ^+ ratio for $\theta^*_\pi \approx 90^\circ$ and 60° plotted versus K in comparison with the σ^{no}/σ^o ratio obtained in this experiment. Although the ratio of σ^{no}/σ^o at 875 mev seems to be a little larger and the ratio at 750 mev seems to be a little smaller than the ratio σ^-/σ^+, the data in general seem to agree with the assumption that both the second and third resonances are dominated by $I \approx 1/2$ state. Certainly the data rule out the possibility of having an $I \approx 3/2$ state dominating in this region which would require the ratio of σ^{no}/σ^o as well as σ^-/σ^+ be equal to one.

Figure 23 shows the $\sigma^D/2\sigma^H$ ratio obtained by Bingham at various angles plotted as a function of K in comparison with the ratio obtained in this experiment. Since only two points can be compared directly, no definite conclusion can be drawn. In general, the data agree within statistics, even though the results of this experiment show a definite tendency to be lower than those of Bingham. The figure also includes the low energy data of Tollestrup et al. (4) on the ratio D/2H.

The cross section for photoproduction of a neutral pion from the neutron as shown in Figure 21 does not show a third resonance. However, the statistical accuracy is too poor and the number of data points too few to draw any definite conclusion.

Contrary to our original hope, no information on the value of angular momentum quantum number is obtained from the experiment due to the scarcity of data points. An order of magnitude improvement on the counting rate must be made before enough data can be obtained in a reasonable amount of time to give information on the value of angular momentum.

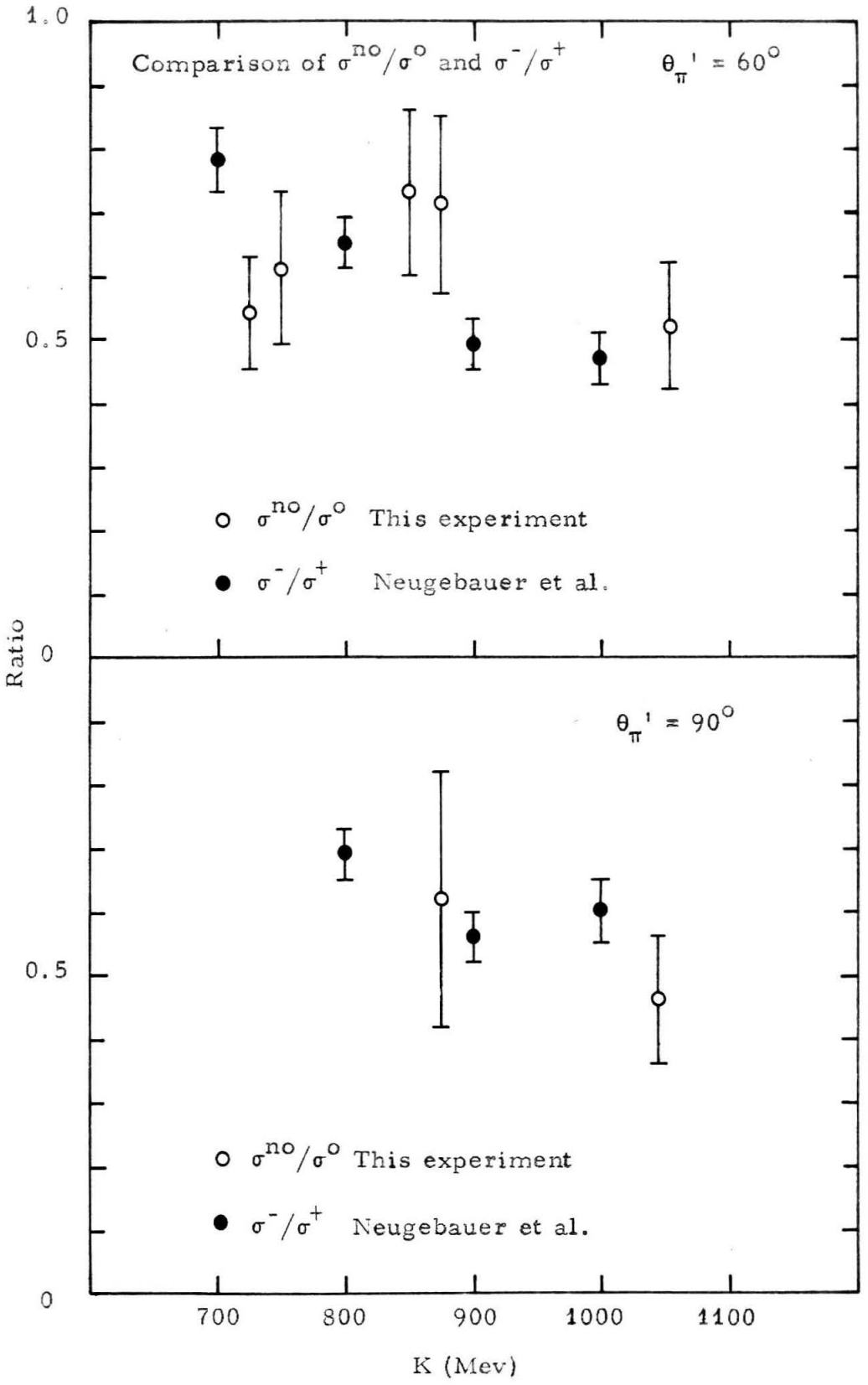
Comparison of σ^{no}/σ^{o} and σ^{-}/σ^{+}
$\theta_{\pi}' = 60^{o}$
σ^{no}/σ^{o} This experiment
σ^{-}/σ^{+} Neugebauer et al.
$\theta_{\pi}' = 90^{o}$
σ^{no}/σ^{o} This experiment
σ^{-}/σ^{+} Neugebauer et al.
Ratio
1.0
0.5
0
0.5
0
700
800
900
1000
1100
K (Mev)

Figure 22

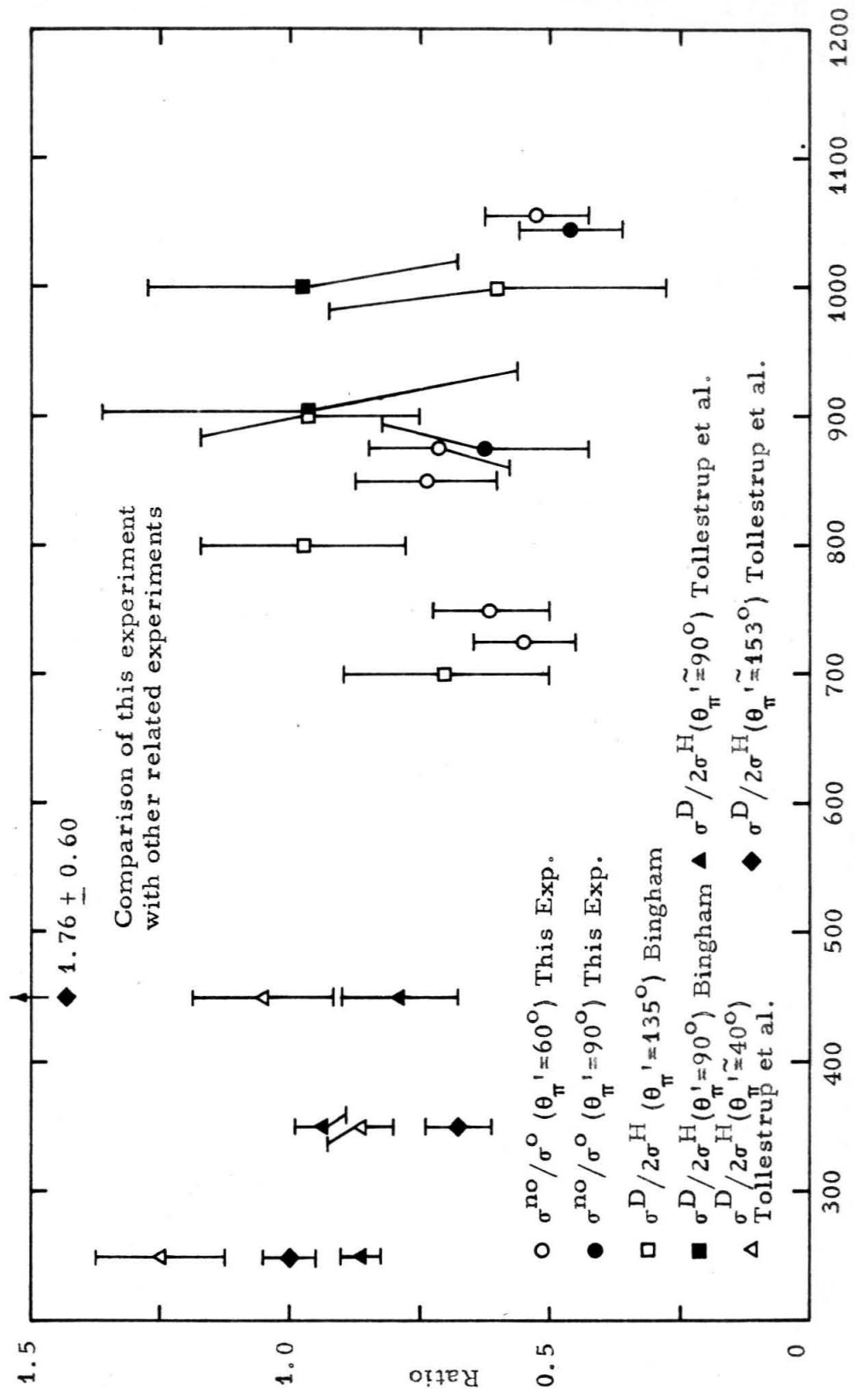
Comparison of this experiment
with other related experiments
◆ 1.76 ± 0.60
○ σ^{no}/σ^{o} ($\theta_\pi' \cong 60^o$) This Exp.
● σ^{no}/σ^{o} ($\theta_\pi' \cong 90^o$) This Exp.
□ $\sigma^{D}/2\sigma^{H}$ ($\theta_\pi' \cong 135^o$) Bingham
■ $\sigma^{D}/2\sigma^{H}(\theta_\pi' \cong 90^o)$ Bingham
▲ $\sigma^{D}/2\sigma^{H}(\theta_\pi' \cong 90^o)$ Tollestrup et al.
△ $\sigma^{D}/2\sigma^{H}(\theta_\pi' \cong 40^o)$ Tollestrup et al.
◆ $\sigma^{D}/2\sigma^{H}(\theta_\pi' \cong 153^o)$ Tollestrup et al.
Ratio
k (Mev)
1.5
1.0
0.5
0
300
400
500
600
700
800
900
1000
1100
1200

Figure 23

The present experiment suffers in the same way as that of Bingham in requiring the use of synchrotron subtraction to determine the energy of the incident photon. In order to avoid using synchrotron subtraction, one must be able to use the fast coincidence circuits as a true time-of-flight instrument. This means that unless a longer time-of-flight path can be obtained together with a correspondingly larger counter to compensate the loss in counting rate the fast coincidence circuits must work well with a resolution time of 2 to 3 nanoseconds independent of the large variations in pulse amplitude. For this to be feasible, one must have a photomultiplier with a rise time of 2 to 3 nanoseconds. The present phototubes have a rise time of 4 to 5 nanoseconds at best. Recently, several new tubes have been manufactured to such specifications. However, they have not been thoroughly tested.

A better way to do this experiment, at least in the forward direction of the outgoing pion, would be to use two lead glass total absorption Cerenkov counters to detect the two photons from the decayed neutral pion. The opening angle of the two lead glass counters would determine the minimum momentum of the neutral pion. The maximum momentum of the neutral pion would be determined by the maximum photon energy of the synchrotron. A large scintillation counter, properly placed, could be used to detect protons. The coincidence of the two lead glass counters and the scintillation counter would indicate the reaction $\gamma + p \rightarrow p + \pi^o$ had taken place while the coincidence of the two lead glass counters alone would indicate the reaction $\gamma + n \rightarrow n + \pi^o$ had taken place. Thus the ratio σ^{no}/σ^o could be measured directly.

APPENDIX I - ESTIMATE OF COUNTING EFFICIENCIES FOR NEUTRONS AND NEUTRAL PIONS

In this section, the ratio of the counting efficiency for neutrons to that for protons and the ratio of the counting efficiency for neutral pions to that for charged pions are estimated.

From the derivation in Section II, we obtain the expressions for the counting rates of the four reactions.

$$C^{no} = A\sigma^{no}\rho^{o}\zeta^{o}\rho^{n}\eta^{no} \tag{1}$$

$$C^{o} = A\sigma^{o}\rho^{o}\zeta^{o}\rho^{p}\eta^{o} \tag{2}$$

$$C^{-} = A\sigma^{-}\rho^{\pm}\rho^{p}\eta^{-} \tag{3}$$

$$C^{+} = A\sigma^{+}\rho^{\pm}\rho^{n}\eta^{+} \tag{4}$$

Since η^{no}, η^{o}, η^{-}, η^{+} have been shown to be equal, we obtain from (3) and (4)

$$\frac{\rho^{n}}{\rho^{p}} = \frac{C^{+}}{C^{-}}\frac{\sigma^{-}}{\sigma^{+}}$$

and from (2) and (3)

$$\frac{\rho^{o}\zeta^{o}}{\rho^{\pm}} = \frac{C^{o}\sigma^{-}}{C^{-}\sigma^{o}} = \frac{C^{o}\sigma^{+}\sigma^{-}}{C^{-}\sigma^{o}\sigma^{+}} = \frac{C^{o}\sigma^{+}C^{-}\rho^{n}}{C^{-}\sigma^{o}C^{+}\rho^{p}}$$

Table 10 shows the values of ρ^{n}/ρ^{p} and $\rho^{o}\zeta^{o}/p^{\pm}$ for the experimental points.

The reason that the values of ρ^{n}/ρ^{p} at points 1, 2, and 3a are larger than those at points 3b, 4, and 5 is probably due to the absorption of the proton by the $1/2^{\pi}$ lead plate. The percentage of proton

Table 10

Ratios of $\frac{\rho^n}{\rho^p}$ and $\frac{\rho^o \zeta^o}{\rho^{\pm}}$

Point	$\overline{K}$ (mev)	θ^*_π	$\frac{\sigma^-}{\sigma^+}$	$\frac{C^+}{C^-}$	$\frac{\rho^n}{\rho^p}$	$\frac{C^o}{C^-}$	$\frac{\sigma^+}{\sigma^o}$	$\frac{\rho^o \zeta^o}{\rho^{\pm}}$
1	1056	60^o	0.42	0.64	0.27	0.56	3.5	0.82
2	876	60^o	0.49	0.51	0.25	0.42	3.4	0.70
3a	749	60^o	0.72	0.57	0.41	0.29	3.2	0.67
3b*	749	60^o	0.72	0.42	0.30	0.26	3.2	0.60
4*	1046	90^o	0.42	0.44	0.19	0.52	1.8	0.39
5*	873	90^o	0.55	0.35	0.19	0.38	1.0	0.21

*No 1/2" lead plate in front of C5.

absorbed, calculated by using geometric cross-section, is approximately 12%. Thus ρ^n/ρ^p will increase from 0.20 to 0.23 if ρ^p decreases from 1.00 to 0.88.

The reason that the value of ρ^n/ρ^p at point 3b is larger than those at points 4 and 5 is probably due to the increase of the neutron efficiency. Figure 24 shows the neutron efficiency as a function of neutron energy (10). Curves for 24 cm and 32 cm scintillators are extrapolated from lower curves. The neutron efficiency for 32 cm scintillator increases from 18% for 300 mev neutrons to 25% for 95 mev neutrons. The average proton energy for point 3b is approximately 150 mev. The lowest proton energy is approximately 110 mev.

Another possible reason for the variation in ρ^n/ρ^p is the relative "scanning efficiencies" for protons and neutrons which vary slightly from point to point. The term "scanning efficiency" is used here to denote the ratio of the number of accepted events which is used in the final results to the total number of events which is the sum of the accepted events and the rejected events due to ambiguous identification.

The values of $\rho^o\zeta^o/\rho^{\pm}$ at points 4 and 5 are approximately 1/2 of the geometric efficiency for counting π^o. This is reasonable because the "scanning efficiency" is only about 60% for π^o. The large value of $\rho^o\zeta^o/\rho^{\pm}$ at points 1, 2, 3a and 3b are due to the large values of ρ^n/ρ^p which come into the expression for $\rho^o\zeta^o/\rho^{\pm}$.

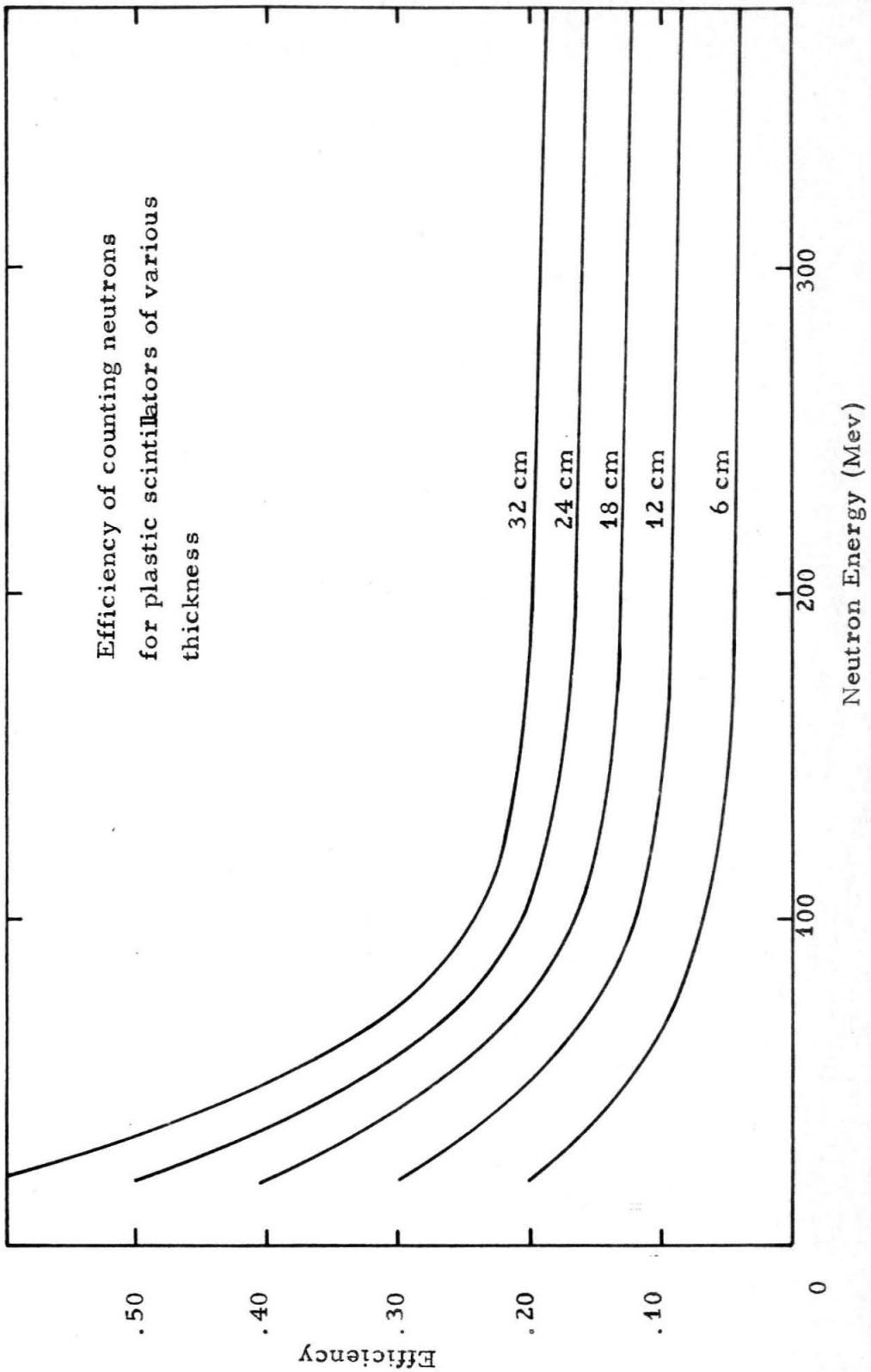
Efficiency of counting neutrons
for plastic scintillators of various
thickness
32 cm
24 cm
18 cm
12 cm
6 cm
.50
.40
.30
.20
.10
0
Efficiency
100
200
300
Neutron Energy (Mev)

Figure 24

APPENDIX II

ESTIMATE OF THE PAIR PRODUCTIONS IN HYDROGEN RUNS

The following pion pair productions from hydrogen are possible.

(1) $\gamma + p \rightarrow p + \pi^+ + \pi^-$

(2) $\gamma + p \rightarrow p + \pi^o + \pi^o$

(3) $\gamma + p \rightarrow n + \pi^o + \pi^+$

The second reaction, when detected, cannot be distinguished from single production of a neutral pion.

The first reaction, when detected, is clearly distinguishable from single production of a pion from hydrogen in this experiment. Chasan et al. (12) give laboratory differential cross sections of this reaction for photons of energies from 500 to 1000 mev. Their results will be used to estimate the $(C_H^{\pm p})_p/(C_H^+)_s$ ratio in hydrogen runs of this experiment.

The third reaction, when neutron and neutral pion are detected, is also clearly distinguishable from single pion production from hydrogen in this experiment. An estimate for the ratio $(C_H^{no})_p/(C^+)_s$ in hydrogen is obtained with the assumption that the ratio of reactions 2 and 3 is given by the isotopic spin relationship given before.

The counting rate for single production of positive pions in hydrogen can be written as

$$(C_H^+)_s = \frac{NW}{E_o}\int_{d\Omega_N}\int_k \sigma^+(\theta'_N)\,(\frac{d\Omega'_N}{d\Omega_N})_s\, d\Omega_N \frac{b(k/E_o)}{k}$$

$$\rho \pm \rho^N \eta^+(k)\epsilon(\theta_\pi)dk$$

$$= B\,\overline{\sigma^+(\theta'_N)}\,(\frac{d\Omega'_N}{d\Omega_N})_s\,\rho \pm \rho^N \Delta\Omega_N\,(\Delta k)_s$$

The counting rate for detecting a charged pion and a proton from pair production in hydrogen is

$$(C_H^{\pm p})_p = \frac{SNW}{E_o} \int_k \int_{P_N} \int_{\Omega_N} \int_{\Omega_\pi} \sigma^{\pm p}(k, \theta'_N, \theta'_\pi\ P'_N)(\frac{d\Omega'_N}{d\Omega_N})_p (\frac{d\Omega'_\pi}{d\Omega_\pi})_p (\frac{dP'_N}{dP_N})_p$$

$$\rho^{\pm}\ \rho^p \eta^{\pm p}\ (k) \epsilon\ (\theta_\pi) d\Omega_N d\Omega_\pi dP_N dk$$

where $\eta^{\pm p}$ is the efficiency of counting the particular pair production determined by the resolution of the coincidence circuits system, and S is the number of possible ways of obtaining the particular pair of final products. For the reaction $\gamma + p \rightarrow p + \pi^+ + \pi^-$, $S = 2$. For the reaction $\gamma + p \rightarrow n + \pi^o + \pi^+$ when the neutron and the neutral pion are detected $S = 1$.

Assuming the angular distribution of the pions is isotropic in the CM system for a given direction of the nucleon, then

$$\sigma^{\pm p}\ (k, \theta'_N, P'_N\ \theta'_\pi) = \frac{1}{4\pi}\ \sigma^{\pm p}\ (k, \theta'_N\ P'_N)$$

$$(C_H^{\pm p})_p = \frac{SNW}{E_o} \int_k \int_{P_N} \int_{\Omega_N} \int_{\Omega_\pi} \frac{\sigma(k, \theta'_N P'_N)}{4\pi} \frac{b(k/E_o)}{k} (\frac{d\Omega'_\pi}{d\Omega_\pi})_p (\frac{d\Omega'_N}{d\Omega_N})_p (\frac{dP'_N}{dP_N})_p$$

$$\rho^{\pm} \rho^p \eta^{\pm p}\ (k) \epsilon\ (\theta_\pi) d\Omega_\pi d\Omega_N dP_N dk$$

$$= B \frac{S}{4\pi} \overline{\sigma^{\pm p}\ (k\ \theta_N\ P_N)} \Delta\Omega_\pi \Delta P_N (\frac{d\Omega'_\pi}{d\Omega_\pi})_p\ \rho^{\pm}\ \rho^p\ \eta^{\pm p}\ (k)\ (\Delta k)_p$$

where $\eta^{\pm p}(k)$ determines the integration limit for dP_N, and as a function of delay T between C5 and C2 is the same as $\eta^+(k)$. Thus

$$\frac{(C_H^{\pm p})_p}{(C_H^{+})_s} = \frac{S\,\sigma^{\pm p}(k, \theta_N, P_N)\Delta\Omega_\pi\,\Delta P_N (\frac{d\Omega'_\pi}{d\Omega_\pi})_p\,\rho^{p}(\Delta k)_p}{4\pi\,\sigma^{+}(k, \theta'_N)(\frac{d\Omega'_N}{d\Omega_N})_s\,\rho^{n}\,(\Delta k)_s}$$

The numerical values for (ΔP_N), $(d\Omega_\pi{}'/d\Omega_\pi)_p$ and $(\Delta k)_p$ can be calculated and $\sigma(k, \theta_N, P_N)\Delta P_N$ can be obtained from Chasan et al.

The exact calculations of the quantities mentioned above are extremely lengthy. For each experimental point, an average for $(d\Omega'_\pi/d\Omega_\pi)_p$ and an average for (ΔP_N) were obtained by calculating $(d\Omega'_\pi/d\Omega'_\pi)_p$ and (P_N) respectively for 240 different configurations, 16 different energies k for the incident photon, and 15 different energies E_π for the detected pion in the laboratory system.

The results of this calculation are shown in Table 11.

Table 11

Calculation for Pion Pair Production in Hydrogen

Point	$(\Delta\Omega_\pi)_p$ (Sr)	$(\frac{d\Omega'_\pi}{d\Omega_\pi})_p$	$(\Delta P_N)_p$ $(\frac{Mev}{c})$	$(\sigma\Delta P_N)_p$ $\mu b/Sr$	$\frac{(\Delta k)_p}{(\Delta k)_s}$	$(\frac{d\Omega'_N}{d\Omega_N})_s$	σ^+ $(\mu b/Sr)$	$\frac{(\rho^\pi \rho^N)_p}{(\rho^\pi \rho^N)_s}$		S		$\frac{(C_H)_p}{(C_H)_s}$	
								$\frac{\pi^{\pm}p}{\pi^+N}$	$\frac{\pi^oN}{\pi^+N}$	$\frac{\pi^{\pm}p}{\pi^+N}$	$\frac{\pi^oN}{\pi^+N}$	$\frac{\pi^{\pm}p}{\pi^+N}$	$\frac{\pi^oN}{\pi^+N}$
1	.083	1.7	510-790	6*	1.8	2.40	5	3.7	0.82	2	1	.07	.003
2	.083	1.7	460-660	8	1.8	2.42	5.3	4.0	0.70	2	1	.10	.004
3	.083	1.7	420-590	7	1.8	2.45	8.2	3.3	0.60	2	1	.05	.002
4	.130	4	600-900	3	1.0	3.20	2	5.3	0.39	2	1	.20	.003
5	.130	4	600-900	3	1.0	3.23	3.0	5.3	0.21	2	1	.14	.001

*The small value of $(\sigma\ P_N)_p$ for point 1 is due to the interpolation of the data of Chasan et al. Their paper gave zero cross section for protons with momentum above 600 $\frac{mev}{c}$ and angle greater than 42^o. Kinematically it is possible to have protons of the above description in pion pair production.

APPENDIX III

ESTIMATE OF THE PAIR PRODUCTIONS IN DEUTERIUM

In this section, the corrections for the pair productions in deuterium are estimated. The quantities to be calculated are f^+, f^-, f^{no}, and f^o as defined in Section VB.

The following expression can be derived from the last equation in Appendix II by proper substitution if the effects of the internal motion of the nucleons in the deuteron are ignored. The definitions of the symbols are also given in Appendix II.

$$f^+ \approx \left[\left(\frac{2}{10} S_3 \, \sigma^{\pm p}(k, \theta_N, P_N) + S_4 \, \sigma^{\pm p}(k, \theta_N, P_N) \right) \right] \frac{\Delta P_N \Delta\Omega_\pi \left(\frac{d\Omega'_\pi}{d\Omega_\pi}\right)_p (\Delta k)_p}{4\pi \, \sigma^+(k, \theta_N) \left(\frac{d\Omega'_N}{d\Omega_N}\right)_s (\Delta k)_s}$$

The first term in the parenthesis represents the contribution from the reaction $\gamma + p \rightarrow n + \pi^+ + \pi^o$ ($S_3 = 1$). The second term represents the contribution from the reaction $\gamma + n \rightarrow n + \pi^+ + \pi^-$ ($S_4 = 2$).

$$f^- \approx \left[\left(S_1 \sigma^{\pm p}(k, \theta_N, P_N) + \frac{2}{10} S_6 \, \sigma^{\pm p}(k, \theta_N, P_N) \right) \right] \frac{\Delta P_N \Delta\Omega_\pi \left(\frac{d\Omega'_\pi}{d\Omega_\pi}\right)_p (\Delta k)_p}{4\pi \, \sigma^-(k, \theta_N) \left(\frac{d\Omega'_N}{d\Omega_N}\right)_s (\Delta k)_s}$$

The first term in the parenthesis represents the contribution from the reaction $\gamma + p \rightarrow p + \pi^+ + \pi^-$ ($S_1 = 2$). The second term represents the contribution from the reaction $\gamma + n \rightarrow p + \pi^- + \pi^o$ ($S_6 = 1$).

$$f^{no} = \frac{4}{10} S_5 \sigma^{\pm p}(k, \theta_N, P_N) \frac{\Delta P_N \Delta\Omega_\pi \left(\frac{d\Omega'_\pi}{d\Omega_\pi}\right)_p (\Delta k)_p}{4\pi \sigma^{no}(k, \theta'_N)\left(\frac{d\Omega'_N}{d\Omega_N}\right)_s (\Delta k)_s} \qquad (S_5 = 2)$$

$$f^{o} = \frac{4}{10} S_2 \sigma^{\pm p}(k, \theta_N, P_N) \frac{\Delta P_N \Delta\Omega_\pi \left(\frac{d\Omega'_\pi}{d\Omega_\pi}\right)_p (\Delta k)_p}{4\pi \sigma^{o}(k, \theta'_N)\left(\frac{d\Omega'_N}{d\Omega_N}\right)_s (\Delta k)_s}$$

The results of this calculation are shown in Table 5 in Section VB.

APPENDIX IV

ESTIMATE OF THE EFFECTS OF WRONG IDENTIFICATION OF REACTIONS

In this section the effects of wrong identification of reactions are estimated. There are four types of possible errors. First, some protons may be identified as neutrons. Second, some neutrons may be identified as protons. Third, some charged pions may be identified as neutral pions. Fourth, some neutral pions may be identified as charged pions.

Let C_o^+ and C^+ be the true and "observed" counting rate of the reaction $\gamma + p \rightarrow n + \pi^+$ where the "observed" counting rate is the counting rate according to our analysis.

Similar definitions are given to C_o^- and C^-, C_o^o and C^o, C_o^{no} and C^{no}.

For the first type of error, let F_{pn} be the fraction of protons wrongly identified as neutrons, then

$$\frac{C_o^{no} C_o^-}{C_o^o C_o^+} = \frac{C^{no} - F_{pn} C^o}{C^o + F_{pn} C^o} \cdot \frac{C^- + F_{pn} C^-}{C^+ - F_{pn} C^-}$$

$$\simeq \frac{C^{no} C^-}{C^o C^+} \left(1 - F_{pn} \frac{C^o}{C^{no}}\right) \left(1 + F_{pn} \frac{C^-}{C^+}\right)$$

$$\simeq \frac{C^{no} C^-}{C^o C^+} \left[1 - \left(\frac{C^o}{C^{no}} - \frac{C^-}{C^+}\right) F_{pn}\right]$$

$$= \frac{C^{no} C^-}{C^o C^+} R_{pn}$$

For the second type of error, let F_{np} be the fraction of neutrons wrongly identified as protons, then

$$\frac{C_o^{no} C_o^-}{C_o^o C_o^+} = \frac{C^{no} + F_{np} C^{no}}{C^o - F_{np} C^{no}} \cdot \frac{C^- - F_{np} C^+}{C^+ + F_{np} C^+}$$

$$\approx \frac{C^{no} C^-}{C^o C^+} \left(1 - F_{np} \frac{C^+}{C^-}\right) \left(1 + F_{np} \frac{C^{no}}{C^o}\right)$$

$$\approx \frac{C^{no} C^-}{C^o C^+} \left[1 - \left(\frac{C^+}{C^-} - \frac{C^{no}}{C^o}\right) F_{np}\right]$$

$$\approx \frac{C^{no} C^-}{C^o C^+} R_{np}$$

For the third type of error, let $F_{\pm o}$ be the fraction of charged pions wrongly identified as neutral pions, then

$$\frac{C_o^{no} C_o^-}{C_o^o C_o^+} = \frac{C^{no} - F_{\pm o} C^+}{C^o - F_{\pm o} C^-} \cdot \frac{C^- + F_{\pm o} C^-}{C^+ + F_{\pm o} C^+}$$

$$\approx \frac{C^{no} C^-}{C^o C^+} \left(1 - F_{\pm o} \frac{C^+}{C^{no}}\right) \left(1 + F_{\pm o} \frac{C^-}{C^o}\right)$$

$$\approx \frac{C^{no} C^-}{C^o C^+} \left[1 - \left(\frac{C^+}{C^{no}} - \frac{C^-}{C^o}\right) F_{\pm o}\right]$$

$$= \frac{C^{no} C^-}{C^o C^+} R_{\pm o}$$

For the fourth type of error, let $F_{o\pm}$ be the fraction of neutral pions wrongly identified as charged pions, then

$$\frac{C_o^{no} C_o^-}{C_o^o C_o^+} = \frac{C^{no} + F_{o\pm} C^{no}}{C^o + F_{o\pm} C^o} \quad \frac{C^- - F_{o\pm} C^o}{C^+ - F_{o\pm} C^{no}}$$

$$\simeq \frac{C^{no} C^-}{C^o C^+} \left(1 - F_{o\pm} \frac{C^o}{C^-}\right) \left(1 + F_{o\pm} \frac{C^{no}}{C^+}\right)$$

$$\simeq \frac{C^{no} C^-}{C^o C^+} \left[1 - \left(\frac{C^o}{C^-} - \frac{C^{no}}{C^+}\right) F_{o\pm}\right]$$

$$= \frac{C^{no}}{C^o} \frac{C^-}{C^+} R_{o\pm}$$

The counting rates of C^-, C^+, C^o, C^{no}, have roughly the ratio of 12 : 6 : 4 : 1. Thus

$$R_{pn} \simeq 1 - (4-2) F_{pn} \simeq 1 - 2 F_{pn}$$

$$R_{np} \simeq 1 - \left(\tfrac{1}{2} - \tfrac{1}{4}\right) F_{np} \simeq 1 - \tfrac{1}{4} F_{np}$$

$$R_{\pm o} \simeq 1 - (6-3) F_{\pm o} \simeq 1 - 3 F_{\pm o}$$

$$R_{o\pm} \simeq 1 - \left(\tfrac{1}{3} - \tfrac{1}{6}\right) F_{o\pm} \simeq 1 - \tfrac{1}{6} F_{o\pm}$$

For the value of $F_{\pm o}$ we use the values of $\frac{N_{123}}{N_{12}}$, $\frac{N_{123}}{N_{13}}$ and $\frac{N_{123}}{N_{23}}$ given in Section V. Since the lower bias for charged pions includes nearly all the charged pions, $1 - \frac{N_{123}}{N_{12}}$ gives roughly the percentage of charged pions giving pulses larger than the upper bias for charged pions set for counter 3. Similar interpretations can be given to the other ratios. Using these ratios, we obtain $F_{\pm o} \approx 0.006$.

For $F_{o\pm}$ we use the value obtained in Appendix V. Thus $F_{o\pm} \approx 0.03$.

For the value of F_{np}, we use the estimate made in Section V.

Thus $F_{np} \approx 0.005$.

The value of F_{pn} depends on the efficiency of counter 4. No estimate based on experimental data can be made. However, the inefficiency of such a counter is generally less than 1%. Thus $F_{pn} \approx 0.01$. Thus we obtain

$$R_{pn} \cong 1 - 2F_{pn} \cong .98$$

$$R_{np} \cong 1 - \tfrac{1}{4}F_{np} \cong .999$$

$$R_{\pm o} \cong 1 - 3F_{\pm o} \cong .98$$

$$R_{o\pm} \cong 1 - \frac{1}{6} F_{o\pm} \cong .995$$

APPENDIX V

ESTIMATE OF THE PERCENTAGE OF THE NEUTRAL PIONS THAT RESEMBLE CHARGED PIONS IN THE PION COUNTER SYSTEM

There is a certain probability that the results of each successive cascade shower initiated by a photon from the decayed neutral pion passing through 1/3 radiation length of paraffin, 2.4 radiation lengths of lead and 1.2 radiation lengths of lead is a single electron. To estimate this correction, we calculate the probability that the number of electrons is 1 after each successive shower. The total probability is then the product of the individual probabilities. For each individual probability, we assume a Poisson distribution for the number of electrons of all energies at depth t in a shower. Let W(N,t) be the probability that the actual number of electrons is N in a given shower at depth t and $\overline{N}(k)$ be the average number of electrons of all energies at depth t in a shower initiated by a photon or electron of a given energy k. Then

$$W(N\,t) = \frac{e^{-\overline{N}}}{N!}\,\overline{N}^{N}$$

N(k) is obtained for lead from Wilson's Monte Carlo calculation (8) and for paraffin from Bernstein's calculation (11). The results are shown in Table 12 where p_1 is the probability that the number of electrons is 1 after a photon passes through 1/3 radiation length of paraffin, p_2 is the probability that the number of electrons is 1 after an electron passes through 2.4 radiation lengths of lead, p_3 is the probability that the number of electrons is 1 after an electron passes through 1.2 radiation lengths of lead, and P is the total probability.

Table 12

PROBABILITY THAT A NEUTRAL PION MAY LOOK LIKE A CHARGED PION IN THE PION COUNTER SYSTEM

Point	p_1	p_2	p_3	P
1	.33	.28	.28	.026
2	.33	.32	.31	.033
3	.33	.35	.32	.037
4	.33	.33	.32	.035
5	.33	.35	.32	.037

REFERENCES

1. Chew and Low, Phys. Rev. 101, 1570 (1956).
2. Chew, Goldberger, Low and Nambu, Phys. Rev. 106, 1337 (1957).
3. Neugebauer, Wales and Walker, Phys. Rev. 119, 1726 (1960).
4. Keck, Tollestrup and Bingham, Phys. Rev. 103, 1549 (1956).
5. H. Bingham, Ph. D. Thesis, California Institute of Technology (1960).
6. J. Boyden, Ph.D. Thesis, California Institute of Technology (1961).
7. Johnson, Bezman, Rubin, Swanson, Corak, and Rifkin, Low Temperature, High Pressure Data of State for Hydrogen and Deuterium between 64 and 300 K, A. E. C. MDDC-850.
8. Wilson, Phys. Rev. 86, 261 (1952).
9. G. Neugebauer, Ph.D. Thesis, California Institute of Technology (1960).
10. Siegel, High Energy Neutron Detectors, Handbuch der Physik, Vol. XLV, Nuclear Instrumentation, Vol. II.
11. Bernstein, Phys. Rev. 80, 995 (1950).
12. Chasan, Cocconi, Cocconi, Schectman, and White, Phys. Rev. 119, 811 (1960).
13. Smythe, Worlock and Tollestrup, Phys. Rev. 109, 518 (1958).
14. Diebold, Gomez, Talman and Walker, Phys. Rev. Letters 7, 323 (1961).
15. Watson, Phys. Rev. 85, 852 (1952).
16. Bingham and Clegg, Phys. Rev. 112, 2053 (1958).
17. Richert and Silverman, Bull. Am. Phys. Soc. 5, 237 (1960).
18. Feldman, Highland, Dewire and Littauer, Phys. Rev. Letters 5, 435 (1960).